SCIENCE CHINA
Information Sciences

• REVIEW •
Special Issue

August 2012 Vol. 55 No. 8: 1722–1754
doi: 10.1007/s11432-012-4633-4

Sparse microwave imaging: Principles and applications

ZHANG BingChen[1,2]*, HONG Wen[1,2] & WU YiRong[1,2]

[1]*Science and Technology on Microwave Imaging Laboratory, Beijing* 100190*, China;*
[2]*Institute of Electronics, Chinese Academy of Sciences, Beijing* 100190*, China*

Received May 10, 2011; accepted June 11, 2012

Abstract This paper provides principles and applications of the sparse microwave imaging theory and technology. Synthetic aperture radar (SAR) is an important method of modern remote sensing. During decades microwave imaging technology has achieved remarkable progress in the system performance of microwave imaging technology, and at the same time encountered increasing complexity in system implementation. The sparse microwave imaging introduces the sparse signal processing theory to radar imaging to obtain new theory, new system and new methodology of microwave imaging. Based on classical SAR imaging model and fundamental theories of sparse signal processing, we can derive the model of sparse microwave imaging, which is a sparse measurement and recovery problem and can be solved with various algorithms. There exist several fundamental points that must be considered in the efforts of applying sparse signal processing to radar imaging, including sparse representation, measurement matrix construction, unambiguity reconstruction and performance evaluation. Based on these considerations, the sparse signal processing could be successfully applied to radar imaging, and achieve benefits in several aspects, including improvement of image quality, reduction of data amount for sparse scene and enhancement of system performance. The sparse signal processing has also been applied in several specific radar imaging applications.

Keywords sparse microwave imaging, sparse signal processing, compressive sensing, synthetic aperture radar, radar imaging

Citation Zhang B C, Hong W, Wu Y R. Sparse microwave imaging: Principles and applications. Sci China Inf Sci, 2012, 55: 1722–1754, doi: 10.1007/s11432-012-4633-4

1 Introduction

Microwave imaging is one of the two main methods of remote sensing, and the other method is optical sensing. The major modern microwave imaging technology in remote sensing is synthetic aperture radar (SAR), which, carries on a platform moving in straight, transmits electromagnetic wave to the scene, receives the radar echo and achieves the high resolution microwave image via signal processing. Comparing with optical sensing technology, SAR is an active sensing technology, and has the all-time and all-weather observing ability. Modern spaceborne and airborne SAR systems have been widely used in such realms as agriculture, forestry, oceanic monitoring, topography mapping and military reconnaissance [1,2].

The concept of SAR was developed by Wiley in 1951 [3,4]. People named this technology as "synthetic aperture radar", because the key point of SAR is to synthesize a large antenna aperture in the azimuth

*Corresponding Author (email: bczhang@mail.ie.ac.cn)

direction by the linear uniform motion of antenna. 1950s–1970s were the origin and early development years of SAR [5]. In 1978, the first spaceborne SAR satellite–SEASAT–was launched [6], which marked a milestone in the SAR development history. SEASAT has a typical resolution of 25 m and swath of 100 km [7]. In the following decades, many more improved SAR systems were developed with much better performance. RadarSat-1 [8] launched in 1995 has a typical resolution of 30 m and swath of 100 km in its standard mode, and TerraSAR-X [9] launched in 2007 has a typical resolution of 3 m and swath of 30 km in typical stripmap mode. Modern SAR systems usually come with high resolution and wide swath with various additional functions such as multi-polarimetric and multi-mode [1,10,11]. As the performance of SAR system improves, the complexity of system also increases remarkably.

In a historic view of SAR development, two key factors determine the SAR system performance: theory of microwave imaging and performance of electronics devices. Theory of microwave imaging was developed at the early 1950s [3,12,13]; it has evolved for over half a century but there is no fundamental revolution. Electronics materials and devices developed rapidly following the Moore's Law [14], which used to be the basis and driving force of the development of microwave imaging system performance during the past decades. The Moore's Law is now facing a bottleneck. The increasing system complexity has brought difficulties to the future evolution of microwave imaging systems.

Two basic laws determine the complexity of a SAR system–the radar resolving theory [15,16] and Nyquist-Shannon sampling theory [17,18]. According to the radar resolving theory, the theoretic resolution upper limit of a radar system is determined by the bandwidth of radar signal. And the Nyquist-Shannon theorem asserts that, the sampling rate must be two times of the signal bandwidth in order to completely recover the origin signal. These two theories together indicate that, as the SAR system performance increases, the sampled data amount will increase remarkably and bring pressure to the system design and implementation.

These two theories are universal, and cannot be overrided. We have to use the specific property of radar imaging system to reduce the complexity of radar system. Since the SAR image is sparse in some special cases, one possible solution is to exploit the sparsity of radar images, introducing the sparse signal processing theory to the radar imaging. Sparse signal processing is developed as a mathematical framework for studying high-dimensional data and uncovering the structures of the data, which is developed by mathematicians at the end of 20th century [19]. Research on sparse signal processing is relatively new, but the idea of it has a long history, which might originate from Ockham's razor "Entities should not be multiplied without necessity" [20]. If the processed signal is sparse, the signal can be measured with dramatically smaller data amount. The recent main achievement of sparse signal processing theory named as compressive sensing (CS), was mainly developed by Donoho, Candès and Tao by the year of 2006 [21–23]. According to the CS theory, under some certain conditions, a sparse signal can be perfectly reconstructed with much less samples than that required by Nyquist-Shannon theory. The CS theory has become the study focus of several fields related to signal processing, such as image processing [24], data compression [25] and communication [26].

Sparse microwave imaging radar, which is a novel strategy of microwave imaging radar, introduces the afore-mentioned sparse signal processing technology to microwave imaging, combines them together to form new theory, new system and new methodology of microwave imaging. Comparing with the traditional SAR, the sparse microwave imaging system might have potential ability to reduce the system data amount and complexity, and potential improvement to the imaging performance. Recent years, plenty of institutes in the world are exploring on the theory and application of sparse microwave imaging radar. Ref. [27] originally suggested applying CS to radar imaging. Refs. [28,29] detailedly analyzed some CS applications to the radar signal processing. Related researches are also carried out in China.

To achieve an applicable sparse microwave imaging system, we must consider four fundamental points [30].

• The mathematical sparse representation of microwave imaging. This is the fundamental question because sparse signal processing theory could only deal with sparse signals.

• The observation constraint condition of sparse microwave imaging and construction of measurement matrix. This question relates to the design of sparse microwave imaging system.

• The unambiguity reconstruction algorithm of sparse microwave imaging with robustness and efficiency. Microwave imaging always faces noise, error and huge data amount.

• The performance evaluation of sparse microwave imaging. We need to develop new evaluation methods to examine the performance of sparse microwave systems.

The rest of this paper is organized as follow. In Section 2, we will refer to the model of traditional SAR and introduce the concept of sparse signal processing and compressive sensing, and then derive the mathematical model of sparse microwave imaging radar system. In Section 3 we will discuss four fundamental points of sparse microwave imaging, including the sparse representation, measurement matrix, unambiguity reconstruction and evaluation methods. We will detailedly elaborate them one by one. An overview of current work on sparse microwave imaging approaches will be provided in Section 4. We point out that, on one hand, current SAR systems can adopt the algorithm of sparse microwave imaging and improve the imaging quality, and on the other hand, new optimized sparse microwave imaging radar system with higher performance can be designed. In Section 5 we will introduce current researches of sparse signal processing and compressive sensing applications in other radar imaging. Finally, the conclusion and future work will be given in Section 6.

2 Modeling of sparse microwave imaging system

In this section, we will provide the derivation of mathematical model of sparse microwave imaging radar. At first we will briefly take the model of traditional SAR and its signal expression as the foundation of following discussions. Then sparse signal processing and compressive sensing theory will be introduced. Finally we will propose the model of sparse microwave imaging radar.

2.1 Synthetic aperture radar model

2.1.1 *Single-channel SAR*

At the beginning of this section, we give a brief description on the single-channel SAR model. Generally speaking, SAR synthesizes the coherent pulses during its integration time to produce high resolution radar images. For different application purposes, SAR has developed many useful operating modes e.g. stripmap, spotlight, ScanSAR and TOPS modes. Since the stripmap SAR is the fundamental and most widely used SAR mode, the following context will discuss the single channel SAR model by taking the stripmap SAR for example.

SAR usually adopts the chirp signal as its transmitting signal:

$$p(\tau) = \mathrm{rect}\left(\frac{\tau}{T_p}\right)\exp\{j\pi K_r\tau^2\}, \quad \tau \in (-T_p/2, T_p/2], \tag{1}$$

where τ is the fast time; T_p denotes time duration of chirp pulse; K_r is the chirp rate; and $\mathrm{rect}(\cdot)$ stands for the unit rectangular function. To the stripmap SAR, the radar platform moves in a straight line, the antenna illuminates the scene and then receives the echo reflected from the observation scene. The geometric relationship can be depicted in Figure 1.

In the case of observing a certain scene C, the echo signal can be written in the form of a double integral [31]:

$$\begin{aligned} s(\tau,\eta) = & \iint_{(x,y)\in C}\sigma(x,y)\cdot w_a\left(\eta-\frac{x}{v}\right)\exp\left\{-j4\pi f_0\frac{R(x,y,\eta)}{c}\right\} \\ & \cdot p\left(\tau-\frac{2R(x,y,\eta)}{c}\right)\mathrm{d}x\mathrm{d}y + N(\tau,\eta), \end{aligned} \tag{2}$$

where η is the slow time; (x,y) is the azimuth and range position of a target; $\sigma(x,y)$ is the backscattering coefficient at (x,y); w_a is the azimuth weighting function; f_0 is the carrier frequency; $R(x,y,\eta)$ is the slant range; v is the equivalent platform velocity relative to the ground; c is speed of light; N is the thermal noise at the receiving terminal. (2) can be simplified into

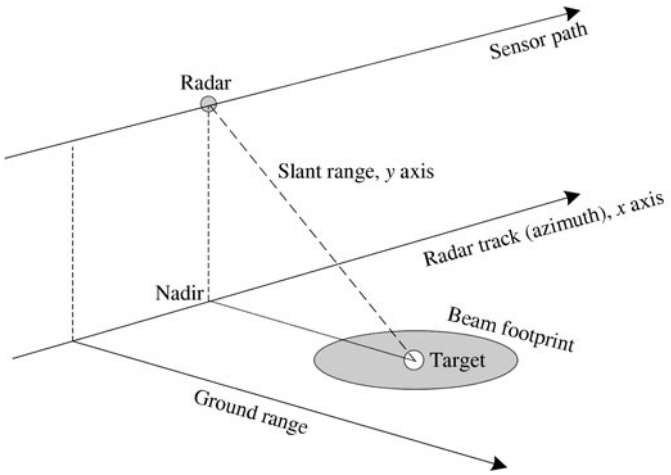

Figure 1 The geometric relationship of stripmap SAR in slant-range plane. The radar platform moves along the sensor path (the x-axis) and illuminates the observation region; the cross track direction (the y-axis) is measured with the slant-range.

$$s(\tau,\eta)=\phi(\tau,\eta,x,y)\otimes\sigma(x,y)+N(\tau,\eta), \tag{3}$$

where $\otimes$ stands for the 2-D convolution; $\phi(\tau,\eta,x,y)$ is the convolution kernel. The $s(\tau,\eta)$ is sampled in discrete form. Let $s[\tau_{m_r},\eta_{m_a}]$ be the m_r-th fast time sample at the m_a-th observation of the echo $s(\tau,\eta)$ and let $\bar{\sigma}[x_{n_r},y_{n_a}]$ be the discrete equivalent backscattering coefficient at the n_r-th position of the slant range and the n_a-th position along the azimuth of the observation scene. Then we can rewrite Eq. (2) as

$$s\left[\tau_{m_r},\eta_{m_a}\right]=\sum_{n_a=1}^{N_a}\sum_{n_r=1}^{N_r}\phi\left[m_a,m_r,n_a,n_r\right]\cdot\bar{\sigma}\left[x_{n_r},y_{n_a}\right]+N\left[\tau_{m_r},\eta_{m_a}\right], \tag{4}$$

where N_a is the number of the discretization cells of scene in slow-time direction; N_r is the number of the discretization cells of scene in fast-time direction.

The conventional SAR imaging algorithms for recovering $\bar{\sigma}[x_{n_r},y_{n_a}]$ use matched filtering method to achieve coherence accumulation. The typical ones among them include the range-Doppler algorithm (RDA), the chirp scaling algorithm (CSA) [32], the $\omega-k$ algorithm [33] and the back-projection (BP) algorithm [34,35].

2.1.2 *Multi-channel SAR*

Multi-channel SAR technology suggests installing more than one transmitting/receiving channels to the SAR platform, and brings potential benefits to the SAR system performance, such as enhancing the system gain, improving system swath and resolution [36–38], reducing the imaging ambiguity, and achieving interferometric and tomographic imaging ability.

A typical multi-channel SAR model is given in Figure 2. Similar to single-channel SAR model, the platform performs a motion with respect to the target scene. The main difference from the single-channel SAR is that more than one receiving channels are installed on the platform. Assume that there are I channels in multi-channel SAR system with one sub-aperture transmitting radar waveform and I sub-apertures receiving echoes. The echo signal of one channel i can be simply derived from the single channel model (2),

$$\begin{aligned}s_i(\tau,\eta)=&\iint_{(x,y)\in C}\sigma(x,y)\cdot w_a\left(\eta-\frac{x}{v}\right)\exp\left\{-j4\pi f_0\frac{R_i(x,y,\eta)}{c}\right\}\\&\cdot p\left(\tau-\frac{2R_i(x,y,\eta)}{c}\right)\mathrm{d}x\mathrm{d}y+N_i(\tau,\eta),\end{aligned} \tag{5}$$

where $i=1,2,\ldots,I$.

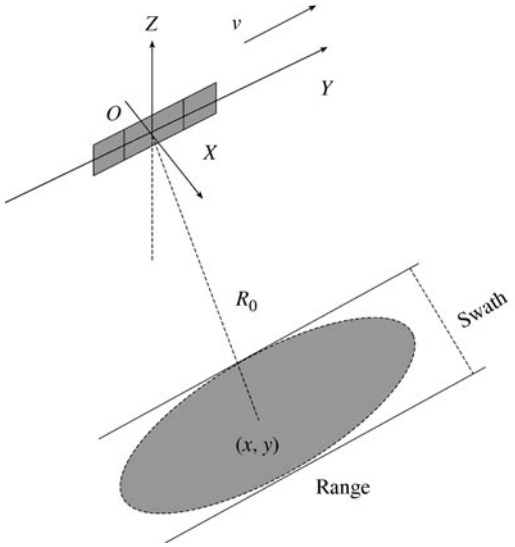

Figure 2 Geometric diagram of multi-channel SAR.

Similarly, we can easily generalize this multi-channel SAR model to multi-transmitting or multi-temporal radar imaging models.

2.2 Sparse signal processing theory

In recent years, a considerable amount of research work has been done on high-dimensional sparse signals. A sparse signal is a signal that can be represented as a linear combination of a few base elements in a basis or an over-complete dictionary [19]. Sparse signal processing focuses on representing the signal in a sparse way so as to make the processing faster and simpler with useful information stored in few coefficients.

According to [39], the history of sparse signal processing can be divided into four stages. First, Mallat et al. [40] introduced the concept of dictionaries to replace the traditional wavelet transform. Second, Chen et al. [41] tackled the quest of the sparsest solution by a convex programming in ℓ_1 norm. Third, a significant step towards a deeper analysis of algorithms and applications in sparse signal processing was made by [41], which proposed the condition that guaranteed the success of sparse signal processing. Last but not least, CS was a crucial stage in sparse signal processing, which was made in 2006 [21]. In the following paragraphs, we will give a brief review of compressive sensing and distributed compressive sensing (DCS).

2.2.1 *Compressive sensing*

CS is related to the problem of how to sample the signal effectively. Essentially, CS is to find a solution for an under-determined linear equation

$$\boldsymbol{y} = \boldsymbol{\Phi x} + \boldsymbol{N}, \tag{6}$$

where measurement matrix $\boldsymbol{\Phi} \in \mathbb{R}^{m\times n}$ satisfies $m < n$, and $\boldsymbol{N}$ is noise. It is well known that if there are fewer equations than unknowns, the equations have either no solution or infinitely many solutions. Nevertheless, unique solution can be obtained under the condition that $\boldsymbol{x}$ is sparse [21,23,42–47] show that suppose $\boldsymbol{x}$ has only s non-zero elements, where s is much smaller than the length of $\boldsymbol{x}$ and matrix $\boldsymbol{\Phi}$ satisfies certain conditions, $\boldsymbol{x}$ can be recovered by

$$\min \|\boldsymbol{x}\|_1 \ \text{ s.t. } \|\boldsymbol{\Phi x} - \boldsymbol{y}\| \leqslant \epsilon. \tag{7}$$

If $\boldsymbol{\Phi}$ is a Gaussian matrix, the recovery of $\boldsymbol{x}$ needs no more than $O(s\log(n/s))$ non-adaptive measurements. The restricted isometric property (RIP) [22] is one of the characteristics describing "good" dictionaries,

which we now define. $\boldsymbol{\Phi}$ is said to satisfy the RIP of order s with parameter δ_s if, for every index set Λ of size s. We have

$$(1-\delta_s)\|\boldsymbol{b}\|_2^2 \leqslant \|\boldsymbol{\Phi}_\Lambda \boldsymbol{b}\|_2^2 \leqslant (1+\delta_s)\|\boldsymbol{b}\|_2^2 \tag{8}$$

for all $\boldsymbol{b} \in \mathbb{R}^s$, where $\boldsymbol{\Phi}_\Lambda$ denotes the submatrix formed by the columns of $\boldsymbol{\Phi}$ indexed by Λ. Signal is not always sparse in the standard coordinate basis. Some orthonormal basis or over-complete dictionary can represent signal in a sparse way, and CS still works. This means that our signal $\boldsymbol{x} \in \mathbb{R}^n$ is now expressed as $\boldsymbol{x} = \boldsymbol{\Psi\alpha}$ where $\boldsymbol{\Psi} \in \mathbb{R}^{n\times d}$ is a dictionary and $\boldsymbol{\alpha}$ is sparse. With (6), we get

$$\boldsymbol{y} = \boldsymbol{\Phi\Psi\alpha} + \boldsymbol{N} = \boldsymbol{\Xi\alpha} + \boldsymbol{N}, \tag{9}$$

where the second equality is by definition of $\boldsymbol{\Xi}$.

2.2.2 *Distributed compressive sensing*

Distributed compressive sensing theory was developed to deal with a signal set [48,49]. In a typical DCS application, a signal set consists of a number of signals. Not only is the redundancy of one signal considered, but also the redundancy of inter-signal correlation structures of the signal set is considered to achieve a compressed sampling strategy. According to the DCS theory, the necessary sampling number is determined by the joint sparsity of the entire signal set, and usually much less than that applying CS to each signal.

Denote the i-th signal by $\boldsymbol{x}_i$ with $i \in \Gamma, i = 1, \ldots, I$, and assume that each signal $\boldsymbol{x}_i \in \mathbb{R}^n$. Then the n-th element of the i-th signal is denoted by $x_i[n]$. Here we assume the signals $\boldsymbol{x}_i$ are sparse and can be measured under CS framework. If the measurement matrix of $\boldsymbol{x}_i$ is $\boldsymbol{\Phi}_i$ and the corresponding measurements are $\boldsymbol{y}_i$, according to CS theory, we have

$$\boldsymbol{y}_i = \boldsymbol{\Phi}_i \boldsymbol{x}_i. \tag{10}$$

In the DCS model, each signal is composed of two components: 1) common components that are shared by each signal; and 2) innovative components that vary among signals. Then, each signal can be expressed as

$$\boldsymbol{x}_i = \boldsymbol{z}_c + \boldsymbol{z}_i, \quad i \in \Gamma, \tag{11}$$

where $\boldsymbol{z}_c$ is the common component which keeps unchanged among channels, and $\boldsymbol{z}_i$ is the innovative component with respect to channel i. If the number of non-zero elements in $\boldsymbol{z}_c$ is much larger than that in $\boldsymbol{z}_i$, and the system has a large joint sparsity, we can use the joint recovery algorithm in the DCS theory to reconstruct the signal set with much fewer samples. A typical scheme diagram of DCS is given in Figure 3.

The overall measurement model of joint processing can be expressed as

$$\boldsymbol{Y} = \begin{pmatrix} \boldsymbol{y}_1 \\ \boldsymbol{y}_2 \\ \vdots \\ \boldsymbol{y}_I \end{pmatrix}, \ \boldsymbol{Z} = \begin{pmatrix} \boldsymbol{z}_c \\ \boldsymbol{z}_1 \\ \vdots \\ \boldsymbol{z}_I \end{pmatrix}, \ \boldsymbol{\Phi} = \begin{pmatrix} \boldsymbol{\Phi}_1 & \boldsymbol{\Phi}_1 & \boldsymbol{0} & \cdots & \boldsymbol{0} \\ \boldsymbol{\Phi}_2 & \boldsymbol{0} & \boldsymbol{\Phi}_2 & \cdots & \boldsymbol{0} \\ \vdots & \vdots & \vdots & \ddots & \vdots \\ \boldsymbol{\Phi}_I & \boldsymbol{0} & \cdots & \cdots & \boldsymbol{\Phi}_I \end{pmatrix}, \ \boldsymbol{Y} = \boldsymbol{\Phi Z}. \tag{12}$$

2.3 Sparse microwave imaging system model

The sparse microwave imaging radar system model is given as

$$\boldsymbol{y} = \boldsymbol{\Phi x} + \boldsymbol{N} = \boldsymbol{\Theta H\Psi\alpha} + \boldsymbol{N}, \tag{13}$$

where $\boldsymbol{x}$ is the back-scattering coefficients of the scene, $\boldsymbol{y}$ is the measured echo data, $\boldsymbol{\Phi}$ is the measurement matrix of radar system , and $\boldsymbol{N}$ is the additive noise. $\boldsymbol{\Phi}$ is defined as $\boldsymbol{\Phi} = \boldsymbol{\Theta H}$ with $\boldsymbol{\Theta}$ being the matrix for the sparse/compressed sampling strategy of the radar echoes, and $\boldsymbol{H}$ being the observation matrix of radar system. The vector $\boldsymbol{x}$ can be decomposed into $\boldsymbol{x} = \boldsymbol{\Psi\alpha}$ with $\boldsymbol{\Psi}$ being a dictionary and $\boldsymbol{\alpha}$ being

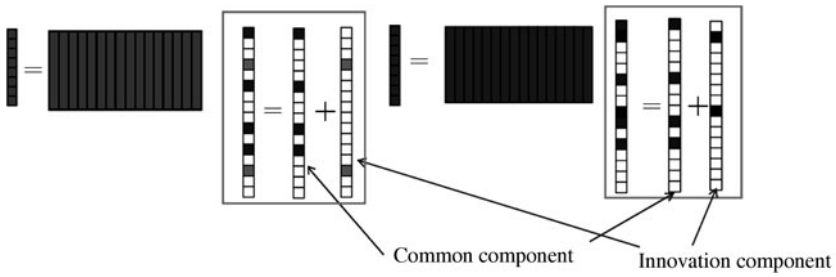

Figure 3 Diagram of DCS approach [48].

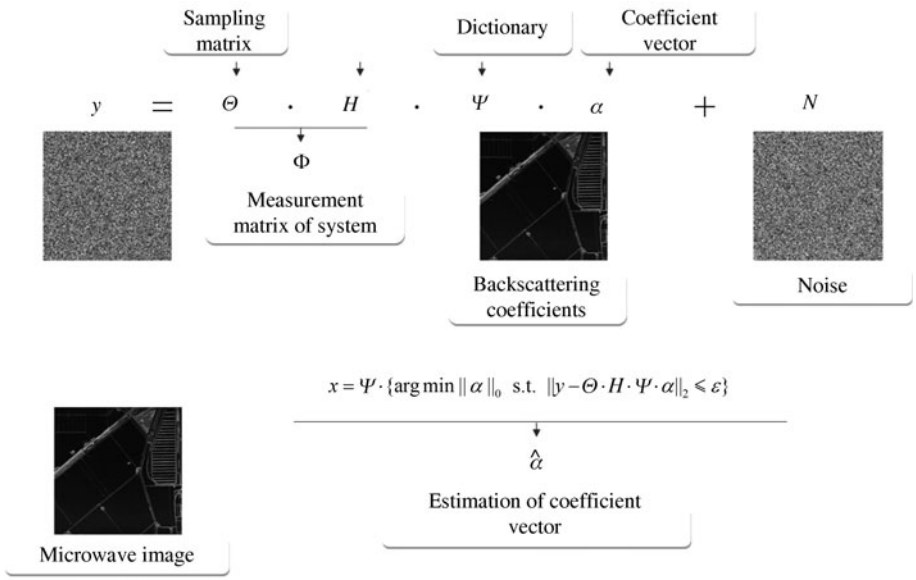

Figure 4 Diagram of sparse microwave imaging radar system model.

corresponding sparse coefficient vector. The diagram of sparse microwave imaging radar system model is given in Figure 4. According to the afore-mentioned sparse signal processing theory, $\boldsymbol{x}$ can be reconstructed by

$$\hat{\boldsymbol{x}} = \boldsymbol{\Psi} \cdot \left\{ \arg\min_{\boldsymbol{\alpha}} \|\boldsymbol{\alpha}\|_0 \ \text{ s.t. } \|\boldsymbol{y} - \boldsymbol{\Theta}\boldsymbol{H}\boldsymbol{\Psi}\boldsymbol{\alpha}\|_2 \leqslant \epsilon \right\}, \tag{14}$$

where $\epsilon = \|\boldsymbol{N}\|_2$. When the observed scene is obviously sparse, the $\boldsymbol{\Psi}$ is chosen as identity matrix, which means it contains only very few dominate scattering targets in the whole scene. In this situation the reconstruction of the scene is given by

$$\hat{\boldsymbol{x}} = \arg\min_{\boldsymbol{x}} \|\boldsymbol{x}\|_0 \ \text{ s.t. } \|\boldsymbol{y} - \boldsymbol{\Phi}\boldsymbol{x}\|_2 \leqslant \epsilon. \tag{15}$$

Combining (4) with (13), the measurement matrix of a typical stripmap SAR can be expressed as [50]

$$\boldsymbol{\Phi} = \begin{pmatrix} \phi_{(1,1)}(1,1) & \dots & \phi_{(X,Y)}(1,1) \\ \phi_{(1,1)}(1,2) & \dots & \phi_{(X,Y)}(1,2) \\ \vdots & & \vdots \\ \phi_{(1,1)}(1,L) & \dots & \phi_{(X,Y)}(1,L) \\ \phi_{(1,1)}(2,1) & \dots & \phi_{(X,Y)}(2,1) \\ \vdots & \ddots & \vdots \\ \phi_{(1,1)}(K,L) & \dots & \phi_{(X,Y)}(K,L) \end{pmatrix}, \tag{16}$$

$$\phi_{(x,y)}(k,l) = w_a\left(\eta_k - \frac{x}{v}\right)\exp\left\{-\frac{4j\pi f_0 R(x,y,\eta_k)}{c}\right\}p\left(\tau_l - \frac{2R(x,y,\eta_k)}{c}\right), \tag{17}$$

where $\tau_l,\ l = 1, 2, \ldots, L$ is the sampling point at range time, $\eta_k,\ k = 1, 2, \ldots, K$ is the sampling time at azimuth time, $x = 1, 2, \ldots, X$ and $y = 1, 2, \ldots, Y$.

3 Fundamental points of sparse microwave imaging

In this section, we will introduce four fundamental points in combining sparse signal processing theory and radar imaging technology. These points cover most aspects of sparse microwave imaging radar system, including the sparse representation, measurement matrix construction, unambiguity reconstruction and performance evaluation.

3.1 Sparse representation

The precondition of applying sparse microwave imaging is that radar image can be represented in a sparse way. In some special cases of microwave imaging, such as inverse SAR (ISAR), tomographic SAR (TomoSAR) and moving target indication(MTI), the observed targets are obviously-sparse. The distribution of ships in the oceans is also obviously-sparse, as shown in Figure 5(a). In these cases, the standard coordinate basis can represent the radar image sparsely. However, the radar image is usually non-sparse, such as image of urban area (see Figure 5(b)). It is important to construct a dictionary which can represent most radar imaging in a sparse way. The aim of sparse representation of radar imaging is to design the corresponding dictionary, so that few coefficients can reveal the information of scene.

Generally speaking, there are two kinds of dictionaries, which are valid in the optical imaging. One is orthogonal dictionary, also called orthogonal basis, which always has minimal size and geometric signal description, such as Fourier bases, cosine bases [51], wavelets bases [52] and so on. The other is redundant dictionary, which usually leads to a better sparse representation, such as tight frame [53], directional wavelet frame [54], curvelet frame [55], adaptive learning dictionary [56] and so on. For the redundant dictionary, more complex algorithms are needed in contrast to orthogonal dictionary.

However, the dictionary mentioned above cannot be directly applied to microwave imaging. Since the backscatter coefficient over uniform regions is complex, and meanwhile the observed in-phase and quadrature components will be independent identically distributed Gaussian random variables [57]. To date, no single dictionary has been deemed as the optimal dictionary for sparse microwave imaging yet. It is still a question and essentially a mathematical challenge for us to optimize the dictionary for microwave imaging.

Eventually, the standard coordinate basis can be applied in the obviously-sparse scene. Moreover, the standard coordinate basis still works in the non-sparse scene, but under a full-sampling scheme, where $\ell_q, q \in (0, 1]$ regularization is applied (see Subsection 3.3).

3.2 Measurement matrix construction

Measurement matrix is the key component of the sparse microwave imaging system model. Nearly all factors of radar system designing can be reflected in the measurement matrix, and its performance directly determines the performance of imaging radar system. As a result, it is important to analyze the main factors and parameters that influence the formation of measurement matrix.

In a mathematical point of view, to a sparse recovering problem, the performance of measurement matrix determines the probability of successfully recovering the signal from the observed data. Mathematicians have found several special matrices which are expected to work well under CS framework, such as random Gaussian matrix [23], Bernoulli matrix [23] and Fourier matrix [44]. Random Gaussian matrix and Bernoulli matrix cannot be directly applied to radar system. If dechirp is applied in the range direction, Fourier matrix can be adopted as measurement matrix [10] in some CS based spotlight SAR approaches [28], but it cannot be applied to stripmap SAR and other SAR imaging modes, nor to matched filtering based spotlight SAR approaches.

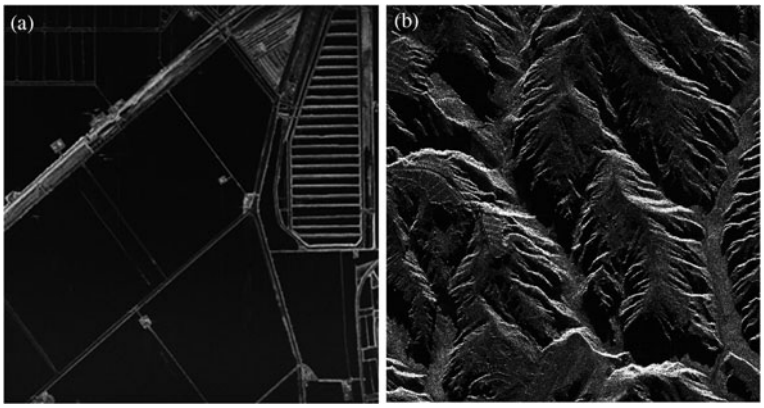

Figure 5 Examples of sparse/non-sparse scenes. (a) Example of obviously sparse scene; (b) example of non-sparse scene.

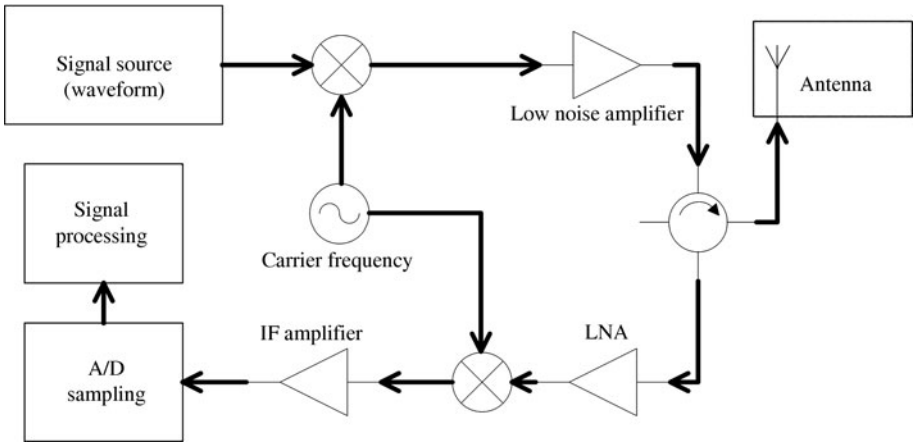

Figure 6 Diagram of components of a radar system [30]. The colored blocks are potentially modifiable.

Obviously, we can directly inherit a traditional SAR system and construct a corresponding measurement matrix, while it is possible to modify the SAR system under the guide of sparse microwave imaging theory and design a measurement matrix with optimized performance. Figure 6 provides a diagram of components of a radar system. In this diagram, we can find some potential modifiable components.

• The waveform. We can modify the radar waveform, thus influencing each element of measurement matrix.

• The A/D sampling. We can apply different sampling strategy under the framework of sparse signal processing to achieve a better measuring effectiveness.

• The antenna spacial location. We can modify the location of antenna, or use an antenna array on the platform. So doing will increase the height of the measurement matrix i.e. more measuring information.

• The antenna footprint. Besides, the platform motion and beam scanning influence the geometric relationship between the antenna and target, and hence the measure matrix.

These factors can be divided into two categories: radar system for the former two components and platform-scene geometric relationship for the latter two. As they determine the construction of measurement matrix $\boldsymbol{\Phi}$. In the rest of this subsection, we will analyze these factors, and discuss the optimized designing of sparse microwave imaging measurement matrix.

3.2.1 *Radar waveform*

Radar waveform design includes the designing of waveform type and waveform band. A well-designed waveform can bring benefits to the increasing of inter-column uncorrelation of measurement matrix and then improve the system performance. In fact, in sparse microwave imaging, each column of the measurement matrix can be treated as a time shift of transmitting waveform.

(i) Waveform bandwidth.

It is difficult to derive an analytical expression of relationship between signal bandwidth and system performance of the sparse microwave imaging system. Generally, a wider signal bandwidth could provide more diversity to the waveform, and higher measurement incoherence. It means that measurement matrix composed of signals with wider bandwidth has better measuring performance. A numerical simulation of waveform bandwidth via phase diagrams indicated that, measurement matrix with a wider bandwidth had a better recovering performance [58].

(ii) Waveform type.

Measurement matrices composed of different waveform types have different measuring abilities. Traditional chirp signal and other waveform types can all be used in sparse microwave imaging, and lead to different system performances.

• Chirp signal.

Chirp signal is widely used in radar systems for its good matched filtering performance and low Doppler sensitivity. It has been broadly applied in traditional radar systems, and could also be applied to sparse microwave imaging systems [27,28,59].

• Orthogonal signals.

Ideal orthogonal signals refer to a signal family $p_i(\tau)$ whose members are orthogonal. The orthogonal signals come in form of a signal family, meaning that the waveform varies in azimuth direction. Expression of orthogonal signals is

$$\int_0^T p_i(\tau)p_j^*(\tau)\mathrm{d}\tau = \begin{cases} 1, & i=j, \\ 0, & i\neq j, \end{cases} \tag{18}$$

where i and j are signal indexes in the family, and $[0,T]$ is the definition domain of signal family.

Measurement matrix composed of orthogonal signals has a higher mutual incoherence and better measuring ability. Here we will discuss two kinds of typical orthogonal signals, namely random noise signals and orthogonal frequency division multiplexing (OFDM) signals.

Random noise signals family is one representative of orthogonal signals. Refs. [60] and [61] researched on the CS based random noise imaging radar.

Another representative of orthogonal signals is the OFDM waveform [62]. A baseband OFDM signal can be expressed as

$$p(\tau) = \sum_{n=0}^{N-1} s_i[n]\exp\{j2\pi n\Delta f\tau\}q(\tau), \tag{19}$$

where N is number of subcarriers, $\Delta f = 1/T$ is the frequency spacing between sequential subcarriers and T is the pulse duration. This ensures that subcarriers are orthogonal to each other. The $q(\tau)$ is a windowing function. Here we use a rectangle window, and denote the data symbols by $s_i[n]$. If the $s_i[n]$ varies during each pulse-repetition time, the OFDM signals also become a signal family. If we do not use the structure of orthogonal subcarriers of the OFDM signals, the OFDM signals perform similarly to random noise signals. Berger et al. studied an application of CS based passive radar using OFDM waveform [63,64].

Ref. [50] compared three types of waveforms via simulation of phase diagram and mean square error. Results showed that random noise and OFDM signals performed much better than the traditional chirp. Other nonlinear FM waveforms can also be applied in sparse microwave imaging.

3.2.2 *Sampling*

Radar signals are continuous analog signals, so the problem of sampling cannot be avoided. The traditional SAR system uses the Nyquist sampling strategy, which causes a huge data amount when signal bandwidth is wide. The sparse signal processing technology gives us the possibility to reduce the sampling rate such that the sampling strategy can be optimized. In the sparse signal processing framework, people have developed several effective sampling schemes. Different sampling strategies lead to different system performances.

The sparse signal processing technology asserts that there exists redundant information in a sparse signal. Usually, a sparse signal has a large bandwidth, but a quite small "information rate" because of its sparseness and redundancy. If we sample the sparse signal with a Nyquist rate, the sampling rate will be quite high and the sampling result will be highly redundant and compressible. As the solution, several new CS based sampling approaches are suggested. People always refer to the CS based sampling approaches as analog-to-information (A2I), which indicates the key point of CS based sampling: the sampling rate is based on information rate of sampled signal, rather than the Nyquist bandwidth criteria [65–68].

Xampling is one of frequently-mentioned CS based sampling framework [69–73]. It is a sub-Nyquist analog-to-digital converter of continuous analog wideband input signal as well as is a non-adaptive sampling framework. The main principle underlying this framework is the ability to process a broad signal model at a low sampling rate. The low rate ADC works in the baseband.

The afore-mentioned CS based analog signal sampling strategies cannot be directly applied to radar devices. These sampling frameworks commonly aim at communication signals, especially wideband communication signals. Such signals are usually sparse in a specific domain, have low information rate, and can be processed with a non-adaptive linear measurement system. But radar signals do not satisfy these conditions.

Usually, radar signals have a high information entropy, so we are not able to apply a linear incoherent measurement directly. But if the scene is sparse, we can treat the target scene as the signal we would like to recover and the observation system as the measurement system, and then achieve some under-sampling strategies. A sparse microwave imaging system tries to reduce the data amount, so the measurement system is usually under-determined and forms an ill-posed problem. A good sampling strategy will improve the performance of measurement matrix and make the recovery problem solvable with an regularization algorithm. Here we will suggest three sampling strategies for sparse microwave imaging: the uniform sampling, the random sampling and the random modulation integral sampling [29,45,74].

(i) Uniform sampling.

As the name suggests, a uniform sampling system has a definite sampling interval. This sampling strategy is simple in hardware implementation, but has a bad performance because the sampling interval keeps invariant in both azimuth and range direction, and brings high mutual coherence to the measurement matrix.

(ii) Random sampling.

The sampling interval changes randomly from one sample to the next in a random sampling scheme. To a random sampling system, the minimal sampling interval might be less than the Nyquist sampling interval, but the average sampling rate might be much less than the Nyquist rate. The sampling interval varies in range and azimuth directions, so the system measurement matrix has a low mutual coherence and a good performance, but such a sampling strategy might bring some difficulties to the hardware implementation. A scheme of random sampling is described in Figure 7.

If we apply random sampling in the azimuth direction, we will encounter a problem of the tradeoff between sampling strategy and swath. As we have known, the azimuth sampling rate, or pulse repetition frequency (PRF), is one key factor that limits the system swath [31]. If random sampling is adopted in azimuth direction, the average sampling rate could be reduced, but because of the randomly chosen instantaneous rate, the minimal sampling interval between sequential azimuth sampling points will also become quite small. In other words, the maximal instantaneous sampling rate will become much higher than average sampling rate. So the radar system swath will be limited.

To solve this problem, people proposed several improved random sampling approaches. For example, the jittered slow-time under-sampling approach [28,75] suggests that the pulse repetition interval (PRI) obeys a uniform distribution around the average PRI. So, a minimal PRI could be guaranteed. Another approach is the so-called Poisson disk sampling strategy [76], which suggests defining the sampling intervals by the sum of a given minimal interval guarantee and a random number obeying uniform distribution in a certain range.

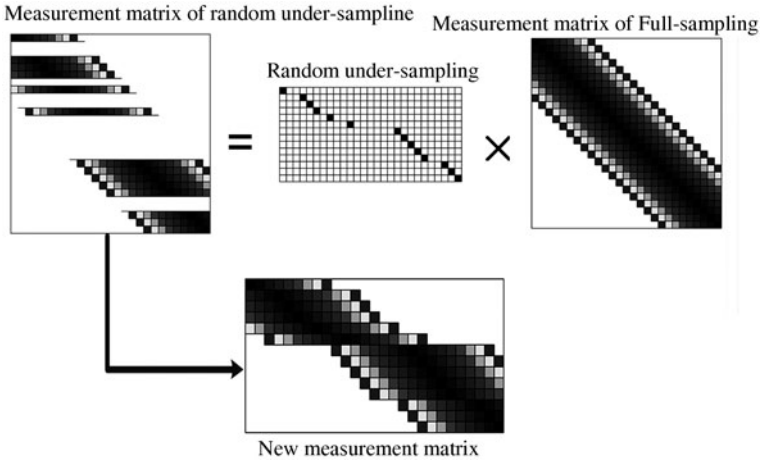

Figure 7 Measurement matrix of random sampling.

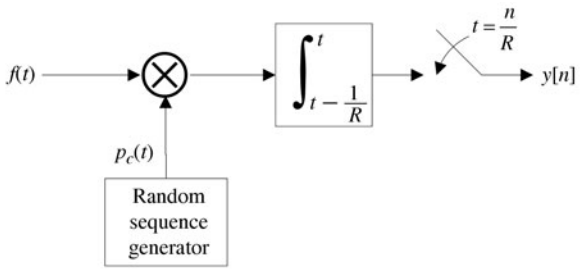

Figure 8 Random modulation integral sampling [77]. The R is sampling number, and n is the index of current sample.

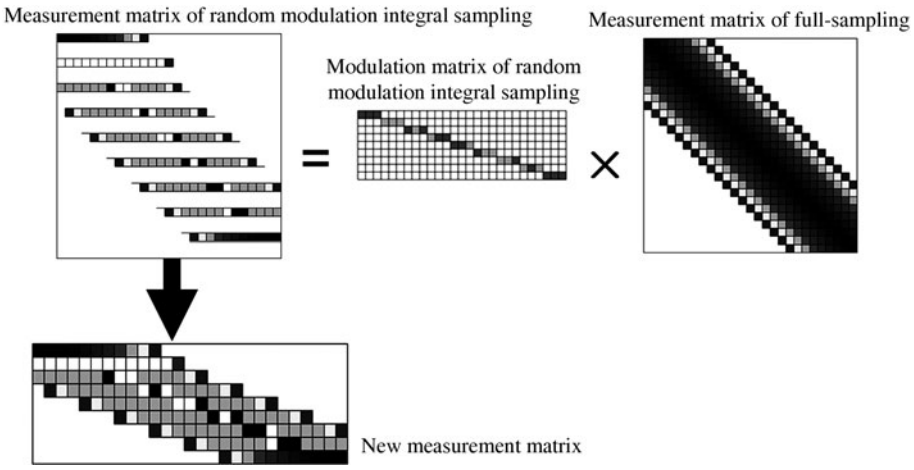

Figure 9 Measurement matrix of random modulation integral sampling.

(iii) Random modulation integral sampling.

In a random modulation integral sampling system, the signals are first modulated and integrated with a random sequence, and then sampled with a uniform sampling system [77]. Simulation results show that random modulation integral sampling has a similar performance to that of the random sampling strategy, and the implementation difficulty of random sampling could be avoided. That is why many A2I approaches suggest using random modulation integral [68,74]. But random modulation integral sampling cannot be applied in the sampling of azimuth. And it is difficult to implement a reliable random modulation integral sampling hardware for wideband radar signal. Scheme of random modulation integral sampling is described in Figures 8 and 9.

3.2.3 *Antenna spacial location*

The instantaneous range distance between the platform and target is a factor that influences the elements in measurement matrix. Such a range distance is determined by the platform-scene geometric relationship. If we make modifications to the geometric relationship and bring more diversity given to it, there might be some potential benefits.

One way to modify the geometric relationship is to alter the antenna spacial location. One antenna could only have one definite location. Some benefits might be achieved when we use more than one transmitting/receiving antennas and apply an antenna array. Besides, different antennas have different geometric locations i.e. different platform-scene relationships. In this situation, each antenna has its own measurement matrix, and the system measurement matrix is combined with these matrices [50].

3.2.4 *Antenna footprint*

The antenna footprint is determined by the platform motion and antenna beam scanning. This is another factor that influences the platform-scene geometric relationship. Traditional SAR requires a linear uniform motion because the synthetic aperture is performed in the azimuth direction. However for sparse microwave imaging radar, the ℓ_q optimization is performed instead of matched filtering, so it is possible to discuss some other motion methods. In the sparse microwave imaging framework, the motion style also determines the instantaneous range distance between the platform and target. If we record the platform's position and velocity in every azimuth sampling point accurately, we can construct a corresponding measurement matrix and recover the scene even if the motion is non-uniform and non-linear. As an extreme situation where multiple antennas were applied, the platform could be stationary. Detailed discussions can be found in [50].

Antenna beam scanning causes variation in the style of radar beam illuminating the targets, and brings change to the formation of measurement matrix. Various antenna bean scanning styles are considered, e.g. stripmap SAR, ScanSAR [31], spotlight SAR [78], sliding spotlight SAR [79,80] and TOPSAR [81].

3.3 Unambiguity reconstruction

The unambiguity reconstruction of sparse microwave imaging employs sparse signal processing algorithms to recover the radar scene, which is different from the traditional matched filtering methods. In the following paragraphs, we will briefly introduce some major sparse signal processing algorithms, and then discuss the problems which occur during applying those algorithms to sparse microwave imaging, including complex data processing, two-dimensional reconstruction and parallel acceleration.

3.3.1 *Sparse signal processing algorithms*

Sparse signal processing algorithms are aiming at solving the linear inverse problem with sparse constraints modelled by

$$\hat{\boldsymbol{x}} = \arg\min_{\boldsymbol{x}} \|\boldsymbol{x}\|_0 \ \text{ s.t. } \boldsymbol{y} = \boldsymbol{\Phi x} \text{ or } \|\boldsymbol{y} - \boldsymbol{\Phi x}\|_2 \leqslant \epsilon, \tag{20}$$

which is a typical combinatorial problem, usually called the ℓ_0-problem [41]. Those algorithms can be classified into several classes: two majors which are usually called "ℓ_1-minimization" and "greedy pursuit" and the others are the "non-convex optimization" and the "Bayesian framework" [82].

ℓ_1-minimization is a class of convex optimization algorithms which replace the ℓ_0-problem with the equivalent ℓ_1-minimization/convex-optimizaton problem [41]. One kind of the ℓ_1-minimization algorithms is based on the interior-point method (IPM), including basis pursuit[41], ℓ_1-regularized least squares (L1-LS) [83], ℓ_1-magic [84], etc. The IPM based algorithms are high order methods, which are accurate but very inefficient for solving large-scale problems. Indeed, they cannot deal with complex variables. The other kind of ℓ_1-minimization algorithms are known as first-order algorithms, including gradient-projected algorithms GPSR [85], SPAGL1 [86], iterative soft-thresholding algorithms ISTA [87], TwIST [88], FISTA [89], Bregman algorithm [90], fixed point algorithms FPC [91], FPC-AS [92], Nesterov based algorithms (NESTA) [93], TFOCS [94], alternating direction methods (ADM) [95,96], etc. The term "first-order"

means that those algorithms only need to calculate the gradient of the optimization function, which are more efficient for solving large-scale problem than IPM based algorithms. As a result, the first-order algorithms are often recommended in recent development of sparse signal processing. The advantage of the ℓ_1-optimization algorithms is that they have a provably accurate recovery when signal is approximately sparse and are robust to the observational noise, while the disadvantage is that most of them are very complicated [97].

Greedy pursuit is a class of non-optimization algorithms that iteratively refine a sparse solution by successively identifying one or more components that exploit the problem structure [40]. Most greedy algorithms are based on the orthogonal matching pursuit (OMP) introduced in [98], which is an improvement of the matching pursuit (MP) algorithm [40]. By adjusting the iterative strategy of OMP, several greedy algorithms are derived, such as the stagewise OMP (StOMP) [99], the gradient pursuit [100], the subspace pursuit [101], the Regularied OMP (ROMP) [102] and the CoSaMP [103]. Except for the OMP based algorithms, the iterative hard thresholding algorithm (IHTA) [104] is also recognized as a greedy pursuit algorithm. The advantage of the greedy pursuit algorithms is that they can be quite fast, especially in the ultrasparse regime, while the disadvantage is that they are inefficient or even invalid when the signal is not very sparse and heavy observational noise is present [82].

Non-convex optimization is the algorithm class which relax the ℓ_0 problem to the related non-convex problem and attempts to identify a stationary point [105]. Some of these algorithms are known as iteratively re-weighted algorithms [105–108]. Besides, the $\ell_{1/2}$ and $\ell_{2/3}$ regularization are demonstrated in [109,110]. The advantage of the non-convex optimization algorithms is that they can deal with less sparse situations than ℓ_1-minimization, whereas the disadvantage is that they are easy to be trapped by the local minimum [105].

Bayesian framework is the algorithm class which assumes a prior distribution for the unknown coefficients that favors sparsity. These algorithms are known as sparse Bayesian learning [111], or Bayesian compressive sensing [112,113]. In addition to these a Bayesian algorithm based on non-convex priori is demostrated in [114]. The Bayesian framework considers the sparse signal processing problem with statistic priori, which is a totally different aspect from the above three classes.

3.3.2 *Sparse signal processing in radar imaging*

Most of the afore-mentioned algorithms can be applied to radar imaging; however, when those algorithms are adopted under the considerations of the characteristics of radar, some efforts should be made to deal with the problem of the complex data processing, the two-dimensional signal reconstruction, and the processing for huge data amount. In the following parts we would like to illustrate these problems in detail.

(i) Complex processing.

There have emerged two methods to treat the complex radar data in sparse signal processing. One is to convert the complex problem into a real problem and solve it by the algorithms of real variables. The other is to solve the complex problem directly.

The former method was widely used in the early stage when the sparse signal processing was applied to the radar imaging [29,115–117], because the complex algorithms had not been well- developed at that time. As a result, the complex radar variables $\boldsymbol{x}$, $\boldsymbol{y}$ and $\boldsymbol{\Phi}$ in (13) had to be decomposed into the real and imaginary parts:

$$\tilde{\boldsymbol{x}} = \begin{pmatrix} \Re\{\boldsymbol{x}\} \\ \Im\{\boldsymbol{x}\} \end{pmatrix}, \ \tilde{\boldsymbol{y}} = \begin{pmatrix} \Re\{\boldsymbol{y}\} \\ \Im\{\boldsymbol{y}\} \end{pmatrix}, \ \tilde{\boldsymbol{\Phi}} = \begin{pmatrix} \Re\{\boldsymbol{\Phi}\} & -\Im\{\boldsymbol{\Phi}\} \\ \Im\{\boldsymbol{\Phi}\} & \Re\{\boldsymbol{\Phi}\} \end{pmatrix}. \tag{21}$$

Then problem of (15) is converted to the following real problem:

$$\arg\min_{\tilde{\boldsymbol{x}}} \|\tilde{\boldsymbol{x}}\|_0 \ \text{ s.t. } \|\tilde{\boldsymbol{y}} - \tilde{\boldsymbol{\Phi}}\tilde{\boldsymbol{x}}\|_2 \leqslant \epsilon_r \tag{22}$$

The latter method emerges while the complex signal processing algorithms have been well-developed. The ℓ_q-minimization algorithms e.g. ISTA, the greedy pursuit algorithms e.g. OMP, and some Bayesian algorithmm have been already applied to radar imaging [118–121].

The disadvantage of the former method is that it doubles the dimension of the unknowns and does not take into consideration that the non-zero real and imaginary components should always occur at the same index. On the contrary, the latter method avoids such disadvantage so that it becomes a better choice in sparse microwave imaging.

(ii) Two-dimensional reconstruction.

In general, with the development in combining the sparse signal processing method with the conventional radar imaging framework, many microwave imaging algorithms have been suggested. The SAR raw data is a two-dimensional signal, the data amount will be huge for current sparse signal processing algorithms. In [59,122], the sparse signal processing is only applied in the range compressed data. Some recent researches reported imaging algorithms that directly applied sparse signal processing to the raw data [118,123]. This kind of methods can be accelerated by decoupling the range and the azimuth of the raw data, as will be introduced in Section 4.

(iii) Parallel acceleration.

Even if the two-dimensional data is processed directly after 2-D decoupling, due to the huge data amount, further acceleration is still required. The performance of algorithm can be enhanced by harnessing the power of graphics process unit (GPU) based parallel computing. GPU-based parallel computing approach has been already introduced to ℓ_1-norm regularization [124–127]. As a research focus, parallel implementation of sparse microwave imaging on GPU clutter needs to be developed.

3.4 Performance evaluation

In this subsection, the evaluation methods for sparse microwave imaging are presented, which consist of the evaluation of radar system performance and image quality.

3.4.1 *Evaluation of radar system performance*

The performance of sparse microwave imaging radar system is mainly related to three factors: sparsity, under-sampling ratio, and signal-to-noise ratio (SNR). Recall equation (13), and assume $\boldsymbol{y}, \boldsymbol{N} \in \mathbb{C}^m$, $\boldsymbol{\Phi} \in \mathbb{C}^{m\times n}$ and $\boldsymbol{x} \in \mathbb{C}^n$. Then the definitions of the three factors are given as follows:

$$\begin{aligned}&\text{sparsity} \triangleq \|\boldsymbol{x}\|_0/n,\\ &\text{under}-\text{sampling ratio} \triangleq m/n,\\ &\text{SNR} \triangleq \|\boldsymbol{\Phi x}\|_2^2/\|\boldsymbol{N}\|_2^2.\end{aligned}$$

In the following paragraphs, we first give a short review of the evaluation criteria for measurement matrix in CS theory, and then introduce the phase diagram which can evaluate the performance of reconstruction. Finally, we propose the performance evaluation method which is suitable to the sparse microwave imaging systems.

In the compressive sensing theory, several criteria are developed to investigate whether the measurement matrix has a good performance for the recovery of the sparse vector, such as restricted isometric property (RIP) [23], restricted orthogonality property (ROP) [42], exact reconstruction criteria (ERC) [128] and mutual coherence [129]. However, in general it is NP-hard to estimate the RIP, ROP and ERC for a given matrix. Mutual coherence is relatively easy to calculate, but the recovery results based on mutual coherence are suboptimal compared with the results on RIP, ROP, and ERC. As a result, these criteria cannot be applied directly in sparse microwave imaging.

Phase diagram [130] is suggested as an evaluation tool of recovery abilities of sparse signal processing. It is a type of chart in physics to describe thermodynamics performance of a material. As a useful tool, Donoho et al. introduced it into the CS theory, to represent the system recovery abilities under different parameter sets of under-sampling ratio and sparsity in a visual intuit chart [131–134].

Phase diagram can be employed to analyze and evaluate the performance of sparse microwave imaging system. The afore-mentioned phase diagram has two axes: sparsity and under-sampling ratio. By comparing the successfully recoverable area of phase diagram under different system conditions, we are

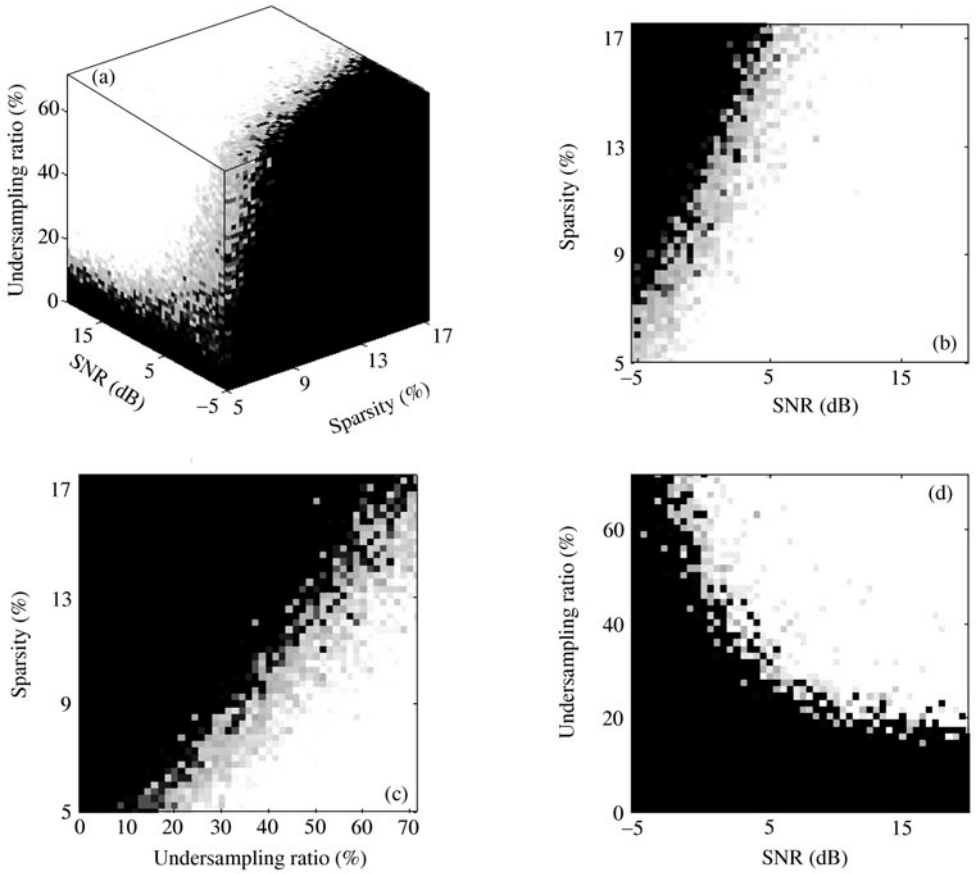

Figure 10 A 3-D phase diagram and 2-D slices. The colors of points in the 3-D phase diagram exhibit the success rates for each combination, where black means the recovery fails, white means the recovery succeeds, and the gray means the recovery partially succeeds. (a) 3-D phase diagram. (b), (c), (d) three slices of the 3-D phase diagram: (b) slice of sparsity/SNR plain (under-sampling ratio=75%); (c) slice of under-sampling ratio / sparsity plain (SNR=5 dB); (d) slice of under-sampling ratio/SNR plain (sparsity=5%). The system parameters: chirp waveform, wavelength = 0.1 m, bandwidth = 50 MHz, pulse duration = 2 μs.

able to evaluate and compare the performances of different systems. Refs. [28,61] have discussed the application of evaluating radar imaging performance using phase diagram.

As an extension, 3-D phase diagram is constructed with one extra dimension–the SNR axis [58], as illustrated in Figure 10.

The advantage of phase diagram is that the performance of system could be displayed visibly and clearly, but its generation requires a large-scale calculation. Moreover, under different waveforms and sampling schemes, the corresponding phase diagrams need to be totally recalculated. A more efficient evaluation tool is required.

3.4.2 *Evaluation of radar image quality*

At present, there does not exist a comprehensive evaluation tool for radar images of sparse microwave imaging. The first problem is the resolving and distinguish ability of point targets. In [135], a fundamental bound of super resolution is given by estimating Cramèr-Rao lower bound for two scatterers. Some papers claim that the super resolution can be achieved in CS based radar imaging approaches [135,136]. The distinguish ability of sparse microwave imaging is studied via simulation and ground-base experiment in [137], which shows that the images of sparse microwave imaging have lower sidelobes. The second problem is the definition of recovery error. [23] suggests adopting mean squared error (MSE) to characterize the recovery error of CS. However, MSE is not suitable for radar images for several reasons, e.g. usually

precise ground truth is not available and the target locating accuracy cannot be sufficiently reflected in MSE.

Under the view of target detection, we can use probability of successful detection P_d and probability of mistaken detection P_e to describe the image recovery quality. But these probabilities are not easy to estimate, and some additional theory is still necessary to be developed.

4 Applications of sparse signal processing in SAR

In this section, we mainly discuss the applications of sparse signal processing in SAR. After reviewing the previous works of CS based SAR imaging, we will give a detailed introduction to the sparse microwave imaging method, including the analysis of SNR, the accelerated algorithm, the reduction of ambiguity and the potential ways of optimizing the hardware system. Finally, we will provide some imaging results on real data which demonstrate the validity of sparse microwave imaging method.

4.1 Current CS based SAR imaging approaches

Ref. [27] presents a compressive sensing based approach of radar imaging, in which the matched filtering is replaced and the required Nyquist sampling rate is reduced to a low "information rate" of the radar reflectivity.

The measurement matrix in spotlight SAR is the Fourier matrix if dechirp is applied. Since the Fourier matrix has good property for compressive sensing recovery [44], CS can be adopted to process the spotlight SAR raw data, as discussed in Section 3. By utilizing the CS theory and the suggested under-sampling strategy, the authors in [28] provide a CS based imaging method and successfully applied it to spotlight SAR imaging.

To stripmap SAR, it is also feasible to use CS based method for range compressed SAR data. A CS based imaging method is proposed in [122], which claims that the randomly under-sampled azimuth data is focused by means of CS instead of the matched filtering methods. Ref. [59] proposes a CS based stripmap SAR imaging scheme, in which the range pulse compression and range cell migration correction (RCMC) are carried out before every azimuth line is recovered by the CS based method. The advantage of these imaging methods is that, as the sparse recovery process only appears in one dimension (often the azimuth dimension), few modifications have been done to the traditional imaging framework and the measurement matrix is not very large.

Recently, there emerges another type of radar imaging methods which directly uses the raw data to recover the images in two dimensions via sparse signal processing [118,138]. Constructing a measurement matrix to deal with two dimensional data is the key step of the method. Under this scheme, the echo data can be under-sampled and no pre-process procedure is required. Thus, the most noticeable advantage is the possibility of simplifying the current imaging radar hardware system, whereas this method demands more computational complexity. In Figure 11, we give the flowcharts of the afore-mentioned imaging methods, with the traditional range-Doppler algorithm as comparison.

4.2 Feasibility and capability of two dimensional recovery

The sparse microwave imaging method aims at recovering the observed scene described in (2) by solving the sparse microwave imaging radar system model (13) with ℓ_q regularization algorithm which has been widely used in sparse signal processing. In this subsection, we firstly present a brief analysis to the SNR of echo signal. The SNR expression reveals the feasibility of SAR imaging from raw data via the sparse microwave imaging method. Since this method demands a considerable amount of storage volume and computational resources due to the immense scale of the measurement matrix, the accelerated algorithm is described in detail to make the ℓ_q regularization method more applicable. The key point of the accelerated algorithm is decoupling the raw data in azimuth and range directions, which is the main factor contributes to the effectiveness of RDA. By using the accelerated algorithm, the ℓ_q regularization

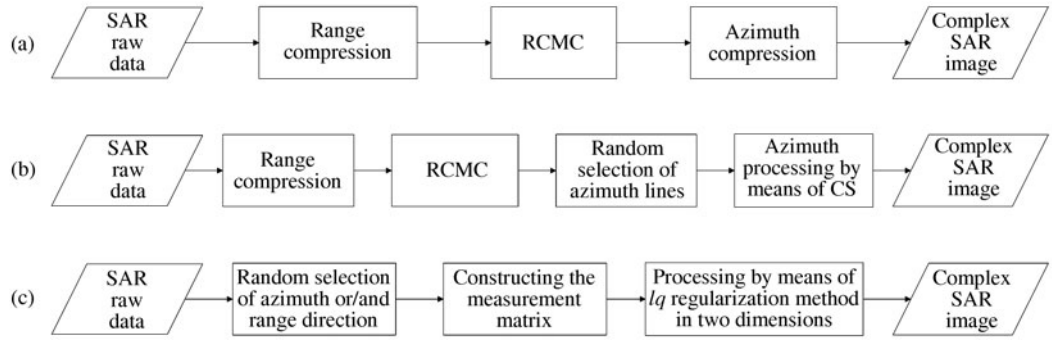

Figure 11 Flowcharts of the imaging methods. (a) Basic RDA; (b) the CS based imaging method in [60,122]; (c) the sparse microwave imaging method mentioned in [118,138].

method can recover the sparse scene with under-sampled raw data, further more, it can also recover the non-sparse scene with full-sampled data. Compared with the traditional matched filtering imaging methods, besides the apparent reduction in sidelobes, the sparse microwave imaging method also shows its ability in reducing the azimuth ambiguity and range ambiguity. The modification of the ℓ_q regularization method for ambiguity reduction is discussed in the third part of this subsection. Finally, we discuss the potential optimization in system design.

4.2.1 *SNR analysis*

The SNR in the echo signal is one of the most important factors that determine the successful recovery rate when the ℓ_q regularization method is used to reconstruct the observed scene. However, according to the traditional radar equation [1], the SNR in the radar echo signal is usually low. In conventional SAR imaging methods, the SNR of point target increases remarkably after the range and azimuth compression, which ensures the high quality radar imaging. As the ℓ_q regularization method directly processes the raw data, it is necessary to analyze the SNR in the echo signal under this framework.

According to (13), the SNR can be defined as $\mathrm{SNR}_{\ell_q} = \|\boldsymbol{\Phi x}\|_2^2/\|\boldsymbol{N}\|_2^2$. In [138], the authors provide a preliminary study on the SNR in the echo signal of CS based SAR imaging, where the extended target is divided into k grids, and it is appropriate to model the radar cross section (RCS) in each grid as a random variable. The authors claim that, if all random variables are independent, the SNR in the echo signal of the extended target can be expressed as

$$\mathrm{SNR}_{\ell_q}^{\mathrm{ext}} = k \cdot \mathrm{SNR}_{\ell_q}^{\mathrm{single}} = k \cdot \mathrm{SNR}_{\mathrm{trad}}, \tag{23}$$

where $\mathrm{SNR}_{\ell_q}^{\mathrm{single}}$ is the SNR of the echo signal of single point target and $\mathrm{SNR}_{\mathrm{trad}}$ is traditional SNR.

On the other hand, if the random variables do not distribute independently, by assuming that $\boldsymbol{\Phi}$ satisfies $\mathrm{RIP}(\mathrm{n}, \mathrm{k}, \delta)$ for every k-sparse vector $\boldsymbol{x}$, the $\mathrm{SNR}_{\ell_q}^{\mathrm{ext}}$ can be expressed as

$$(1-\delta)\frac{E(\|\boldsymbol{x}\|_2^2)}{E(\|\boldsymbol{N}\|_2^2)} \leqslant \mathrm{SNR}_{\ell_q}^{\mathrm{ext}} \leqslant (1+\delta)\frac{E(\|\boldsymbol{x}\|_2^2)}{E(\|\boldsymbol{N}\|_2^2)}. \tag{24}$$

Ref. [138] also provides some simulations which demonstrate the validation of this expression. Under most circumstances, the SNR is enough for successful recovery via ℓ_q regularization.

4.2.2 *Accelerated algorithm*

The key point of accelerating the ℓ_q method is to decouple the raw data into two respective dimensions as reported in [123] and Fang et al's paper[1)]: the azimuth and range. Then either of them can be processed by ℓ_q regularization with much smaller scale. This idea is inspired by range cell migration correction (RCMC). To apply the acceleration, we introduce the "SAR raw data simulators" which is just the back-

1) Fang J, Xu Z B, Zhang B C, et al. Fast compressed sensing SAR imaging based on approximated observations. IEEE Trans Geosci Remote Sens, Submitted

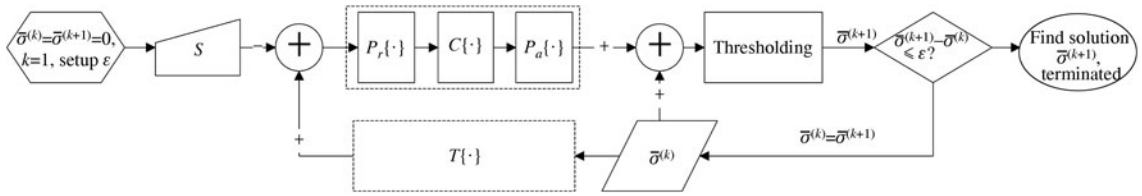

Figure 12 Flowchart of decoupling.

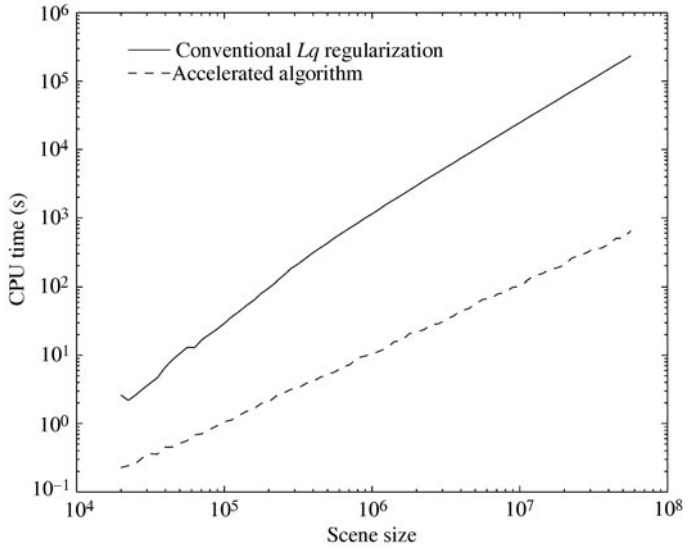

Figure 13 Computing time cost comparison (log-log scale).

ward procedure to the traditional matched filtering method. Let $T\{\cdot\}$ be the SAR raw data simulator, given by

$$S = \Theta T\{\bar{\sigma}\}. \tag{25}$$

Taking RDA for example, the basic steps of the RDA include range compression, RCMC and azimuth compression. Let P_r be the operator of the range compression, P_a be the operator of the azimuth compression and C be operator of the RCMC. The procedure of range cell migration is the inverse of C; thus, T can be expressed as

$$T\{\cdot\} = P_r{}^*\{C^{-1}\{P_a{}^*\{\cdot\}\}\}. \tag{26}$$

Then, the accelerated algorithm can be written as

$$\min_{\bar{\sigma}}\{\|S - \Theta P_r{}^*\{C^{-1}\{P_a{}^*\{\bar{\sigma}\}\}\}\|_2 + \lambda\|\bar{\sigma}\|_q^q\}, \tag{27}$$

where $*$ denotes adjoint operator and -1 denotes inverse operator. The flowchart of the accelerated algorithm is shown in Figure 12.

Decoupling of the data aims at trade-off between accuracy and efficiency. By applying the accelerated algorithm, the computational complexity can be reduced from square order to linear logarithm order [123], as shown in Figure 13. From the above description, we can see that the accelerated algorithm is the integration of ℓ_q method and the traditional frequency operation, so this algorithm can be used in reconstruction of not only sparse scenes but also non-sparse scenes.

4.2.3 *Reduction of ambiguity*

The sparse microwave imaging method can be used to reduce the azimuth ambiguity and range ambiguity in SAR imaging [139][2),3)] and improve the image quality of current SAR systems.

- Azimuth ambiguity reduction.

2) Fang J, Xu Z B, Zhang B C, et al. Azimuth ambiguity suppression in SAR based on extended Doppler observation. IEEE Trans Signal Process, Submitted

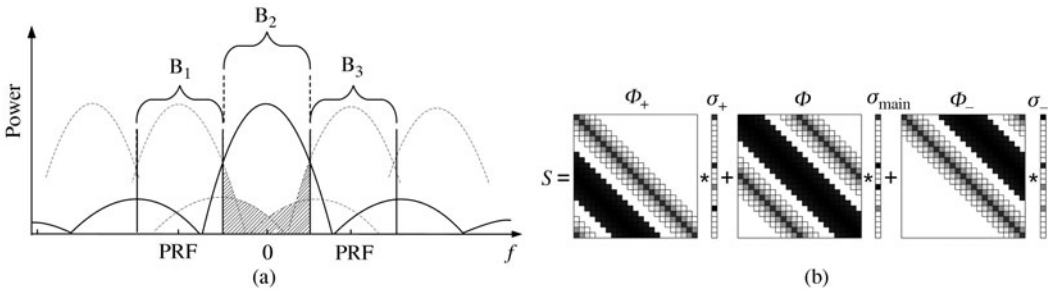

Figure 14 Illusion of azimuth ambiguity. (a) The signal components (B_1 and B_3) outside the main frequency intervals B_2 holds back into the main part of the spectrum [1]. (b) As a result, the echo data can be divided into three parts which belong to the corresponding lobes.

The azimuth ambiguity arises from the finite sampling of the Doppler spectrum at intervals of PRF. Since the spectrum repeats at PRF intervals, the signal components outside this frequency intervals hold back into the main part of the spectrum. Due to this reason, the ambiguity power in time domain appears similar to the original target except the amplitudes experience slight loss. Figure 14 illustrates the cause of azimuth ambiguity [1]. In general, there exist difficulties in reducing the ambiguity power under the framework of the traditional imaging methods. However, the azimuth ambiguity can be reduced by applying some modifications to the sparse microwave imaging radar system model (13). To be concise, we mainly focus on reducing the first sidelobe of antenna pattern since it contributes most of the ambiguity components. Let $\boldsymbol{x}_{\text{main}}$ be the backscattering coefficient; let $\boldsymbol{x}_+$ and $\boldsymbol{x}_-$ be the ambiguity components brought by the first sidelobes of the antenna pattern. Then the echo $\boldsymbol{y}$ in (13) is the sum of three parts:

$$\boldsymbol{y} = \boldsymbol{\Phi}_+\boldsymbol{x}_+ + \boldsymbol{\Phi}\boldsymbol{x}_{\text{main}} + \boldsymbol{\Phi}_-\boldsymbol{x}_-. \tag{28}$$

$\boldsymbol{\Phi}_+$ and $\boldsymbol{\Phi}_-$ are the corresponding measurement matrix of ambiguity components. $\boldsymbol{\Phi}_+$ and $\boldsymbol{\Phi}_-$ have the same arrangement of $\phi_{i+}(k,l)$ and $\phi_{i-}(k,l)$ as (16), where

$$\phi_{i+}(k,l) = w_a(\eta_k + \text{PRF}/K_a)\exp\left\{-4j\pi f_0\frac{R(i,\eta_k+\text{PRF}/K_a)}{c}\right\}p\left(\tau_l - \frac{2R(i,\eta_k+\text{PRF}/K_a)}{c}\right), \tag{29}$$

$$\phi_{i-}(k,l) = w_a(\eta_k - \text{PRF}/K_a)\exp\left\{-4j\pi f_0\frac{R(i,\eta_k-\text{PRF}/K_a)}{c}\right\}p\left(\tau_l - \frac{2R(i,\eta_k-\text{PRF}/K_a)}{c}\right). \tag{30}$$

$$\boldsymbol{y} = \begin{bmatrix} \boldsymbol{\Phi}_+ & \boldsymbol{\Phi} & \boldsymbol{\Phi}_- \end{bmatrix} \cdot \begin{bmatrix} \boldsymbol{x}_+ \\ \boldsymbol{x}_{\text{main}} \\ \boldsymbol{x}_- \end{bmatrix} = \boldsymbol{\Phi}_{\text{ambi}} \cdot \boldsymbol{x}_{\text{ambi}}. \tag{31}$$

Then the above $\boldsymbol{x}_{\text{ambi}}$ can be solved by an ℓ_q regularization algorithm.

$$\min_{\boldsymbol{x}_{\text{ambi}}} \left\{ \|\boldsymbol{y} - \boldsymbol{\Phi}_{\text{ambi}}\boldsymbol{x}_{\text{ambi}}\|_2 + \lambda\|\boldsymbol{x}_{\text{ambi}}\|_q^q \right\}. \tag{32}$$

We are interested in $\boldsymbol{x}_{\text{main}}$, which is the ambiguity reduced image. Details of azimuth reduction based on sparse microwave imaging can be found in Fang et al's paper[2)].

• Range ambiguity reduction.

The range ambiguity is due to the echoes from preceding and succeeding pulses that arrive at the antenna simultaneously with the desired return. The model of sparse microwave imaging can also be adopted to decrease the range ambiguity by similar approaches as reported in our paper[3)].

3) Zhang B C, Hong W, Wu Y R, et al. A radar imaging range ambiguity reducing method based on ℓ_q regularization (in Chinese). China Patent. Submitted

4.2.4 *Design of novel system*

The sparse microwave imaging method has potential ability in improving the imaging quality of current radar systems. After the initial concept of sparse microwave imaging has been fully tested with simulated and real data, more ambitious radar system could be designed, which would rely on the sparse sampling scheme to achieve wider swath and higher imaging performance.

The oceanic scene are usually assumed to be sparse when the clutter noise is omitted. Since the sparse microwave imaging method can directly process the under-sampled echo data of sparse scenes to recover the radar image without loss in imaging quality, the requirement of Nyquist sampling rate can be relaxed. Thus, it is possible to obtain a much wider swath by applying slow-time under-sampling strategy and the sparse microwave imaging method. On the other aspect, the sparse microwave imaging method provides a potential way to acquire better distinguish ability.

The design of high performance sparse microwave imaging radar involves sparse signal processing, radar system designing and sparse microwave imaging evaluation. The related work is in progress by the authors and will be presented in the future.

4.3 DCS based multi-channel SAR imaging

In the multi-channel microwave imaging applications, it is possible to apply DCS theory to achieve some benefits in the reduction of data amount and increment of imaging performance. As we have mentioned in (5), the echo of multi-channel SAR model is different among different channels. In [140], the authors indicate that, if there exist position changes and elevation changes in the target points during the observation, the echo of each channel will have an extra phase $\boldsymbol{\beta}_i$ which varies among different channels. Denote

$$\boldsymbol{x}_i(x,y) = \boldsymbol{\sigma}(x,y)\exp\{\boldsymbol{\beta}_i\}, \tag{33}$$

the $\boldsymbol{x}_i(x,y)$ is the targets needed to be recovered and can be expressed in the form of DCS

$$\boldsymbol{x}_i(x,y) = \boldsymbol{z}_i(x,y) + \boldsymbol{z}_c(x,y), \tag{34}$$

where $\boldsymbol{z}_i(x,y)$ is the innovation part among signals of different channels, which is brought by the $\boldsymbol{\beta}_i$. If the observation time duration is not very long, the $\boldsymbol{\beta}_i$ might not be very large and most of $\boldsymbol{z}_i(x,y)$ should be zero. In this condition, the signals of different channels have a large joint sparsity and DCS can be applied to reduce the data amount.

In [141], DCS is applied to a multi-channel along-track interferometric (ATI) application to achieve the moving target indication (MTI). In ATI model, antenna channels are installed in the azimuth moving direction. The moving targets in the scene bring phase variations to different channels, i.e. the innovation components. Simulations show that, under specific circumstances, DCS based MTI approach with the under-sampling rate of 10% could achieve similar indication performance with DPCA approach. If we simply apply CS but not DCS to each channel the recovery is not successful.

DCS could also be applied to scene change detection [142]. The approach is quite similar. The radar observes the same scene for multiple times in a multi-pass model, while echo of each pass forms a channel. If the change in scene during various observations is not significant or abroad, the innovation components among different channels should be sparse, and as a result DCS is applicable.

DCS is a useful technology in many applications. It might have potential applications on not only moving target indication and change detection, but also on radar imaging models where inter-channel redundancies exists, such as antenna array, MIMO radar and beamforming.

4.4 Experimental results

4.4.1 *Simulations*

In [138], the authors present a series of experiments on 2-D simulated data to demonstrate that the sparse microwave imaging is capable of recovering the sparse scene with under-sampled raw data. The first conclusion reached by the authors is that the results by the ℓ_q regularization contain less artifacts

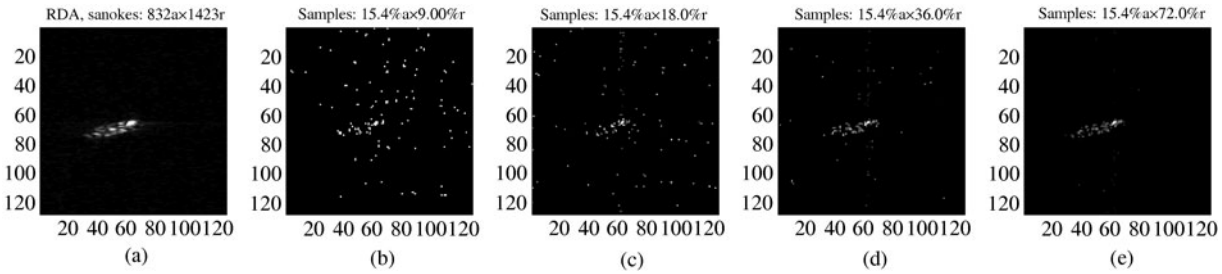

Figure 15 Imaging results on a ship target, RadarSat-1 by the Sparse Microwave Imaging method with different under-sampling rate. The result on the same target by RDA taken with full-sampled data as comparison. (a) Imaging result by RDA with full-sampled raw data; (b) imaging result by sparse microwave imaging with 1.38% of under-sampled raw data; (c) imaging result by sparse microwave imaging with 2.77% of under-sampled raw data; (d) imaging result by sparse microwave imaging with 5.54% of under-sampled raw data; (e) imaging result by sparse microwave imaging with 11.1% of under-sampled raw data.

than that by the traditional method and the sidelobes is lower as well. The second conclusion is that the amplitude and phase of the results exhibit a more precise matching to the ground truth while the SNR increases. It means that the ℓ_q regularization algorithm can preserve the phase information of the radar image.

4.4.2 *Imaging with real data of sparse scene*

The sparse microwave imaging method is also capable of recovering the scene from real SAR data. For sparse scene, the sparse microwave imaging method can use the under-sampled raw data to produce the high quality radar images. The first set of imaging results we provide here is a part of Figure 5(a), shown in Figure 15. The results indicate that, as the under-sampling rate increases from 1.38% (b) to 11.1% (e), the artifacts in the imaging results by the sparse microwave imaging method decrease and the ship becomes clearer. The sidelobes in Figure 15(e) is lower than the imaging result by RDA in Figure 15(a).

4.4.3 *Imaging with real data of non-sparse scene*

On the other hand, by employing ℓ_q regularization as the recovery algorithm, the sparse microwave imaging method leads to successful imaging for non-sparse scene with full-sampled measurements. In Figure 16, we provide some imaging results on the urban area by the ℓ_q regularization algorithm. It is shown that the sidelobes of those strong targets are reduced. Moreover, the details of the land are clearer in the Figure 16(c) than in Figure 16(b) which is imaged with RDA.

4.4.4 *Ambiguity reduction*

Besides the improvement in sidelobe reduction, the sparse microwave imaging method can be used to reduce the ambiguity noise[2)]. In Figure 17, the simulation results of ambiguity reduction on one-point target show that, by applying the sparse microwave imaging method, the peak of the azimuth ambiguity power decreases by about 22 dB. This ambiguity reduction approach can be applied to real SAR data.

5 Sparse signal processing in various radar applications

As a research focus of recent years, the sparse signal processing theory, especially compressive sensing has also been broadly used in various radar related applications. In this section, we will provide an overview of these approaches of introducing CS to related applications, including tomographic SAR (TomoSAR), inverse SAR (ISAR), ground penetrating radar (GPR)/through-the-wall radar imaging (TWRI), wide angle SAR (WSAR)/circular SAR (CSAR), multi-input multi-output (MIMO) radar, moving target indication (MTI) and SAR data compression.

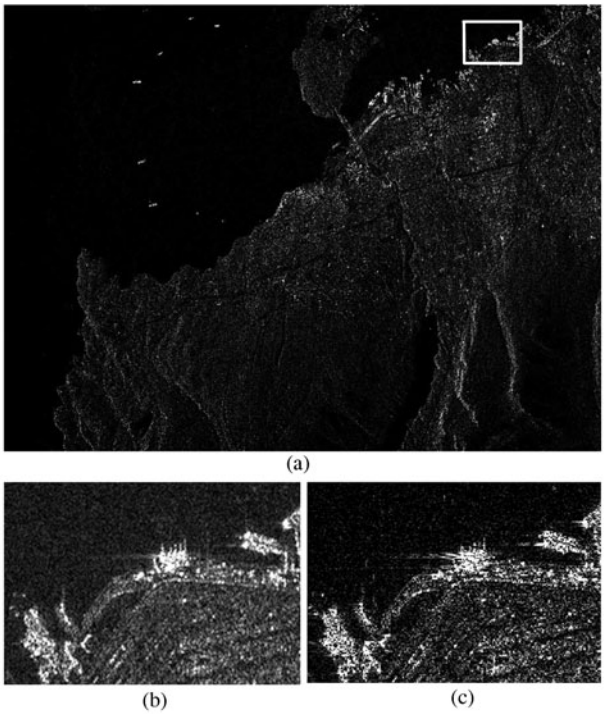

Figure 16 Imaging result on the urban area. Data is acquired with RADARSAT of area in Vancouver, Canada. (a) Imaging result by the sparse microwave imaging method with full-sampled raw data; (b) result of white rectangular area by RDA with full-sampled raw data; (c) result of white rectangular area by sparse microwave imaging method with full-sampled raw data.

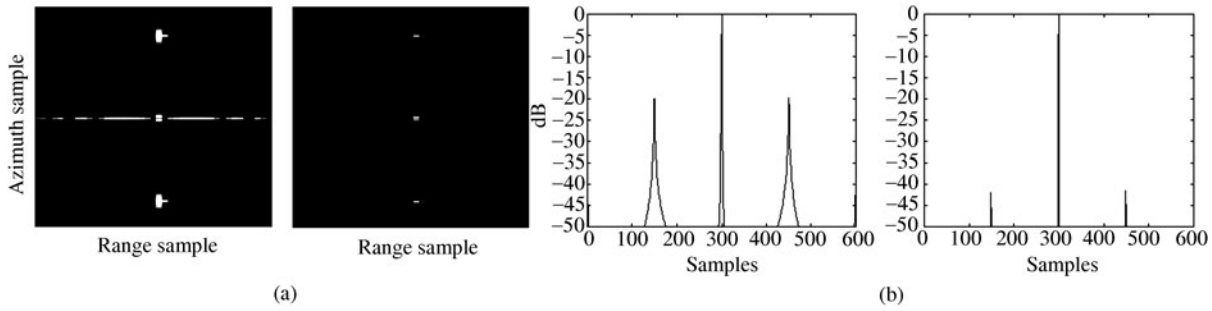

Figure 17 Results of ambiguity reduction simulation on one-point target by the sparse microwave imaging method with full under-sampled data, with the result by RDA with full under-sampled data taken as comparison. (a) Left: Amplitude of the result by RDA; right: amplitude of the result by the sparse microwave imaging method; (b) left: the normalized amplitude in the range cell that contains the point target, by RDA, where the peak of the ambiguity power is −20 dB; right: The normalized amplitude in the range cell that contains the point target, by the sparse microwave imaging method, where the peak of the ambiguity power is −42 dB.

5.1 Tomographic SAR

Tomographic SAR (TomoSAR), also named as three-dimensional SAR (3D-SAR), is a newly developed technology which expands the traditional 2-D SAR imaging to a 3-D imaging system [143–145]. Traditional SAR and interferometric SAR (InSAR) do not have the distinguishing ability along the elevation dimension, so it is not able to deal with tomographic problems such as shadowing and overlays. TomoSAR has a 3-D point spread function, so it has distinguish ability in all three dimensions and makes it possible to solve the afore-mentioned problems. However, in real applications, it is difficult to acquire enough data to get a high resolution in the elevation dimension. But usually, there do not exist many objects in one azimuth-range cell along the elevation dimension, i.e. there exists a sparse representation in the elevation direction. So the sparse signal processing is applicable here in TomoSAR imaging.

Several efforts have been made to apply sparse signal processing to TomoSAR imaging, and many compressive sensing based algorithms have been applied in the real data processing of TerraSAR-X [146], COSMO-SkyMed [147], ERS1/2 [148] and GOTCHA [119] datasets. Ref. [149] suggested that CS based tomographic imaging is feasible. As the authors indicated, modern satellite orbits were tightly controlled, so the tomographic resolution was highly limited; the data amount was also a limitation. Based on the fact, authors developed the so-called SL1MMER (scale-down by ℓ_1 norm minimization model selection estimation reconstruction) algorithm [150] and applied it to TerraSAR-X dataset [146]. The super resolution ability is also discussed [135,151,152], and such method was applied to 4D-SAR applications, which also considered "time" as one dimension [146]. Similar work was reported in reference [148], where the authors discussed a TomoSAR application based on multi-pass signal model. Comparing with the conventional Fourier-based method which was suffering from large data amount requirement and irregular sampling space, a novel method based on CS and ℓ_1 regularization was suggested, and such method was verified on an ERS1/2 dataset. Alike, [147] applied the CS-based method to COSMO-Skymed dataset, and compared the CS based method with statistical tomography method.

Other researchers and institutes also worked on the CS based TomoSAR imaging. Ref. [153] indicated that the major advantages of the proposed CS-based method over other conventional methods were evident in single snapshot scenarios with correlated scattering components. Ref. [119] applied CS-based tomographic method to the GOTCHA Air Force Research Laboratory (AFRL) dataset, which consists of multi-pass complete circular aperture radar data. Ref. [154] provided CS based TomoSAR signal model and sampling constraint conditions, and discussed its applicability via simulations.

5.2 Inverse SAR

Inverse synthetic aperture radar (ISAR) is a version of SAR that can be used operationally to image targets such as ships, aircrafts, and space objects with high resolution by utilizing the movement of the targets rather than the radar platform to create the synthetic aperture [155]. The sparse signal processing can be applied to ISAR because there are only a few dominant point-like scattering centers that ensure the sparsity condition.

In [29], CS based ISAR technique is applied to image TIRA (tracking and imaging radar) system satellites. Ref. [28] employed sparse signal processing technique to ISAR imaging and validated it with experimental data. Ref. [121] presented an ISAR imaging method for the moving train with a remarkable reduction in the A/D requirement. In a series of work of sparse ISAR imaging [120,156–159], the authors investigated several different compressed ISAR measurement realizations, i.e. the measurement with limited pulses, with sparse probing frequencies, with sparse apertures, and developed high-performance algorithms for sparse ISAR imaging. In these works, all the system designs and the algorithms were validated from the real data of Yak plane. The authors proposed a data compression framework of ISAR by transforming the echo signal to spectrogram plane in [160], and reported a high resolution ISAR imaging method with sparse stepped-frequency waveforms in [161]. An ISAR enhancement technology based on CS is mentioned in [162]. In [163], the ISAR problem for uniformly rotation targets is solved in the context of sparse signal recovery via parametric weighted ℓ_1 minimization.

5.3 Ground penetrating radar and through-the-wall radar

Ground penetrating radar (GPR) is an important observation and detecting technology which is designed primarily for the location of objects or interfaces buried beneath the Earth's surface or located within a visually opaque structure [164,165]. GPR is widely applied in variety of areas such as civil engineering, landmine detection, archaeological and other environmental applications [166]. Traditional GPR images the ground surface by scanning the sensor over the interested region, transmitting short pulses and processing the echo. Such echo data can be processed with several imaging algorithms in time domain or in Fourier domain [167,168], while all these algorithms require large data amount and well-sampled signals, which brings difficulties to the data acquisition of GPR systems.

Gurbuz et al. suggested that the CS based GPR imaging is applicable when the target scene is sparse, i.e. there only exist a small number of point targets [166,169,170]. The authors indicated that, the

dictionary of GPR data can be created by discretizing the target space, and synthesizing the GPR model data for each discrete spatial position. Different from traditional Nyquist sampling, the measurement was applied by taking linear projections of random sampled echo signal with random vectors. They applied such CS based GPR scheme to simulated and experimental GPR data. The results showed that the data amount reduced remarkably, and the target images were less cluttered than conventional imaging results.

Different from afore-mentioned common impulse GPR, another type of GPR–stepped-frequency continuous-wave (SFCW) GPR–becomes increasingly popular these years. The SFCW GPR observes the scene with a discrete set of frequencies and synthesizes the impulse in the frequency domain [165], and brings advantage of better measuring accuracy. In [171,172], Suksmono et al. introduced CS to the SFCW GPR system. They pointed out that, the CS measurement could be done in the frequency domain by randomly measuring all Fourier coefficients. Gurbuz et al. also paid attention to CS based SFCW GPR [173], and indicated that the CS based SFCW GPR had the super resolution ability compared to standard schema via experiments.

The system of Through-the-Wall Radar imaging (TWRI) is quite similar to GPR; as a result, CS is also introduced to TWRI. Ref. [117] presented a novel CS based TWRI system, which applied CS to the data acquisition scheme and remarkably increased the data acquisition efficiency. Its applicability is proved via simulations and real system experiments. Similar work is proposed in [174].

5.4 Wide angle SAR and circular SAR

Wide angle synthetic aperture radar (WSAR) refers to any synthesized aperture whose angular extent exceeds the sector required for equal resolution in range and cross-range. Although the wide angle SAR provides an optical-like image that is more readily recognized and interpretable, standard SAR imaging formation algorithms, such as polar-format algorithm, fail to completely realize the potential of wide angle SAR for the anisotropic of targets. Sparse signal process theory can be applied in WSAR to solve this problem. In [175], WSAR imaging is modelled as a sparse inverse problem over an over-complete dictionary, with a dictionary element representing a prescribed reflectivity signature of a spatial pixel in the azimuth direction. By exploiting the correlations in target reflectivity and the spatial sparsity of target scattering, a similar dictionary approach is given in [176]. In addition, this approach keeps valid even if the data is sub-sampled.

Circular SAR (CSAR) takes a circular motion trace and observes the target scene from all directions [177]. CSAR has a three-dimensional point spread function, so it has a 3-D imaging ability. Ref. [178] introduced a CS based imaging of a vehicle from eight passes with 360 degrees apertures. Lin et al. applied CS to Circular SAR (CSAR) imaging in [179,180]. Their work aimed at the sidelobe reduction using CS and ℓ_1 regularization in CSAR application. They verified the applicability of the algorithm via an in-lab experiment of imaging a human body [180].

5.5 MIMO radar

Multiple-input multiple-out (MIMO) radar system is characterized by transmitting and receiving multiple independent, usually orthogonal waveforms via its antennas simultaneously [181,182]. MIMO technology is also applied to SAR system [183], which combines the independent echo signals in a diversity gain, enables MIMO SAR system to improve the resolution and target identifiability. Due to successful application of compressive sensing in traditional radar system to reduce the sampling rate, people also introduced CS to MIMO radar.

In [184], the authors pointed out that, in CS based MIMO radar, if the target signals were sparse, the compressive sensing technology could be used to reconstruct the scene in the azimuth-range-Doppler domain. A waveform design method to reduce the inter-target correlation was also introduced. Similar work was presented in [185], where the authors also validated the theoretical performance bounds via numerical simulations. [186,187] detailedly proposed works on MIMO radar using CS, where the direction of arrival (DOA) estimation ability of CS based MIMO radar was discussed, and indicated that, if the targets were located sparsely in the angle-Doppler space, approaches based on CS and ℓ_1 regularization could be applied to achieve super resolution with much fewer samples than that required by other

approaches. Ref. [188] studied measurement matrix design of CS based MIMO radar, where optimal measurement matrix design was discussed with the optimality criterion depending on the coherence of the sensing matrix (CSM) and/or signal-to-interference ratio (SIR). Ref. [189] introduced a CS based approach to accurately estimate the parameters of multiple targets and analyzed the performance of MIMO radar system. Ref. [190] introduced the sparse learning via iterative minimization (SLIM) to MIMO radar signal processing, and indicated that SLIM followed an $\ell_q(0 < q \leqslant 1)$ constraint and provided more accurate estimations than ℓ_1-regularization based approaches. In [63,191] the authors mainly presented their work on the CS based passive radar with OFDM waveform. Ref. [192] investigated MIMO imaging radar, and derived principle of CS MIMO imaging radar based on inverse scattering model instead of conventional geometric model in an ISAR application.

5.6 Moving target indication

Moving target indication (MTI) is a mode of radar operation to discriminate a target against stationary clutter. After removing the background, moving targets are sparse in the velocity/position domain. Recently, sparse signal processing technology has been introduced into MTI to estimate both the positions and velocities of moving targets with moving targets sparsely distributed in the observed scene. Approaches of CS based MTI are introduced in [193,194]. DCS based multi-channel MTI is reported in [140,141]. Through adaptive nulling techniques in the spirit of space-time adaptive processing (STAP), multiple-phase center antennas suppress clutter and produce a moving target indication image [178]. An over-complete dictionary inversion approach based on CS theory is presented to simultaneous imaging of stationary and moving scatterers [195]. 3-D moving-target-imaging approach is also discussed as a particularly difficult sparse-aperture imaging problem in [196].

5.7 SAR data compression

In SAR imaging, the raw data amount is always huge and brings extra difficulty to data storing and downlink. Mainly because of the high entropy of SAR raw data, it is very difficult to achieve an effective SAR data compression [197]. The most widely used traditional SAR raw data compression method, block adaptive quantization (BAQ), is based on quantization, which is a lossy compression strategy [198]. As the Compressive Sensing has been successfully applied to optical imaging compression, efforts have been made to compress SAR raw data via CS. An encoding algorithm based on compressed sensing to compress the SAR data was presented in [199,200]. The algorithm represents the SAR data using real wavelets and then decodes with the OMP algorithm.

Ref. [194] discussed an compression method of processed SAR images of MiniSAR using curvelet sparsity-promoting CS recovery in offline decoding.

6 Conclusions and future work

There exists much progress in the efforts of combining sparse signal processing with the microwave imaging and applying novel methods in radar imaging. However, many problems have been met during such efforts and in order to solve the problems, the research on fundamental theories of sparse microwave imaging needs to be strengthened and more work on the system design and experimental validation of sparse microwave imaging should be done.

1. There remain several fundamental questions on the theoretical side of sparse microwave imaging. First, how to characterize and describe the sparsity of target scattering in the view of electromagnetic scattering mechanism? This determines the applicability condition of sparse microwave imaging. Second, can we find a comprehensive theory to analyze the mechanism of sparse microwave imaging? We need a theoretical tool to describe the sparse microwave imaging, ensuring its effectiveness and guiding its designing. Information theory should be a candidate method, since it has been used to analyze the radar resolving problem [15], and has also been adopted to analyze performance of CS in recent years [201–203]. In sparse microwave imaging, the information theory might have potential applications in describing and

analyzing the performance bounds of radar systems. Some preliminary researches have been reported in [137].

2. How to construct the optimal measurement matrix for sparse microwave imaging under the guide of sparse signal processing theory? This question is still not clear because we have not achieved a practical method to assess the recovery ability of measurement matrix of the sparse microwave imaging system. Several factors determine the structure of measurement matrix, such as the sampling waveform, strategy, antenna location, antenna footprint, transmitting power, etc. Under the constraints of system designing requirement, we should optimize these factors in order to construct a good measurement matrix.

3. Recovery algorithm with efficiency and robustness needs to be developed for the large data amount, non-negligible noise level and inevitable system error of sparse microwave imaging. To achieve efficiency, we should accelerate the ℓ_q regularization recovery algorithms by introducing the specificity of radar imaging into sparse signal processing. Furthermore, the recovery algorithm should be stable in the presence of noise and modelling errors. We need to analyze the performance of recovery algorithms under the non-ideal conditions.

4. How to evaluate the performance of sparse microwave imaging? This is also an open problem. The evaluation includes evaluation of radar system performance and evaluation of radar image quality. To the radar system performance evaluation, we need to develop an evaluation tool with more efficiency than that of the phase diagram. To evaluate the quality of the radar image, there does not exist a comprehensive evaluation method yet.

Sparse microwave imaging is a novel concept and is a focus of remote sensing. It has attracted considerable research interest in recent years. Sparse microwave imaging is believed to bring remarkable changes to the technology of remote sensing in the future.

Acknowledgements

This work was supported by National Basic Research Program of China (Grant No. 2010CB731900).

References

1 Curlander J C, McDonough R N. Synthetic Aperture Radar: Systems and Signal Processing. New York: Wiley, 1991
2 Henderson F M, Lewis A J. Principles and applications of imaging radar. In: Manual of Remote Sensing. New York: John Wiley and Sons, 1998
3 Wiley C, Ariz P. Pulsed Doppler Radar Methods and Apparatus. US Patent 3,196,436. 1965
4 Wiley C A. Synthetic aperture radars: a paradigm for technology evolution. IEEE Trans Aerosp Electron Syst, 1985: 21: 440–443
5 Wikipedia. Synthetic Aperture Radar. https://en.wikipedia.org/wiki/Synthetic_aperture_radar
6 NASA. Missions–Seasat 1. http://science.nasa.gov/missions/seasat-1/
7 Jordan R L. The Seasat-A synthetic aperture radar system. IEEE J Ocean Eng, 1980, 5: 154–164
8 CSA. CSA: RadarSat-1. http://www.asc-csa.gc.ca/eng/satellites/radarsat1/
9 DLR. TerraSAR-X-Germany's radar eye in space. http://www.dlr.de/eo/en/desktopdefault.aspx/tabid-5725/9296_read-15979/
10 Jakowatz C V, Wahl D E, Eichel P H, et al. Spotlight-Mode Synthetic Aperture Radar: A Signal Processing Approach. Norwell: Kluwer Academic Publishers, 1996
11 Massonnet D, Souyris J C. Imaging with Synthetic Aperture Radar. Lausanne: EFPL Press, 2008
12 Brown W M, Porcello L J. An introduction to synthetic-aperture radar. IEEE Spectrum, 1969, 6: 52–62
13 Sherwin C W, Ruina J P, Rawcliffe R D. Some early developments in synthetic aperture radar systems. IRE Trans Military Electron, 1962, 1051: 111–115
14 Moore G E. Cramming more components onto integrated circuits. Electron Mag, 1998, 86: 82–85
15 Woodward P M. Probability and Information Theory, with Application to Radar. New York: Pergamon, 1953
16 Cook C E, Bernfeld M. Radar Signals-An Introduction to Theory and Application. Norwood: Artech House, 1993
17 Nyquist H. Certain topics in telegraph transmission theory. Trans Amer Inst Electr Engin, 1928, 47: 617–644
18 Shannon C E. Communication in the presence of noise. Proc IRE, 1949, 37: 10–21
19 Baraniuk R G, Candès E, Elad M, et al. Applications of sparse representation and compressive sensing. Proc IEEE, 2010, 98: 906–09

20 Russell B. History of Western Philosophy. London: George Allen & Unwin Ltd, 1946
21 Donoho D L. Compressed Sensing. IEEE Trans Inf Theory, 2006. 52: 1289–1306
22 Candès E J, Tao T. Near-optimal signal recovery from random projections: Universal encoding strategies? IEEE Trans Inf Theory, 2006, 52: 5406–5425
23 Candès E J, Romberg J K, Tao T. Stable signal recovery from incomplete and inaccurate measurements. Commun Pure Appl Math, 2006, 59: 1207–1223
24 Mallat S, Yu G. Super-resolution with sparse mixing estimators. IEEE Trans Image Process, 2010, 19: 2889–2900
25 Zhang Y, Mei S, Chen Q, et al. A novel image/video coding method based on compressed sensing theory. In: Proc of IEEE International Conference on Acoustics, Speech and Signal Processing (ICASSP), Las Vegas, 2008. 1361–1364
26 Berger C R, Zhou S, Preisig J, et al. Sparse channel estimation for multicarrier underwater acoustic communication: from subspace methods to compressed sensing. IEEE Trans Signal Process, 2010, 58: 1708–1721
27 Baraniuk R, Steeghs P. Compressive radar imaging. In: Proc of IEEE Radar Conference, Boston, 2007. 128–133
28 Patel V M, Easley G R, Healy D, et al. Compressed synthetic aperture radar. IEEE J Sel Top Signal Process, 2010, 4: 244–254
29 Ender J H G. On compressive sensing applied to radar. Signal Process, 2010, 90: 1402–1414
30 Wu Y R. Studies on theory, system, and methodology of Sparse Microwave Imaging. Statement Tasks and Project Plan of 973 Program: 2009
31 Cumming I G, Wong F H. Digital Signal Processing of Synthetic Aperture Radar Data: Algorithms and Implementation. Norwood: Artech House, 2004
32 Raney R K, Runge H, Bamler R, et al. Precision SAR processing using chirp scaling. IEEE Trans Geosci Remote Sens, 1994, 32: 786–799
33 Bamler R. A comparison of range-Doppler and wavenumber domain SAR focusing algorithms. IEEE Trans Geosci Remote Sens, 1992, 30: 706–713
34 Basu S, Bresler Y. $O(N^2 \log_2 N)$ filtered backprojection reconstruction algorithm for tomography. IEEE Trans Image Process, 2000, 9: 1760–1773
35 Xiao S, Munson Jr D C, Basu S, et al. An $N^2 \log N$ back-projection algorithm for SAR image formation. In: Conference Record of Asilomar Conference on Signals, Systems and Computers (ACSSC), Pacific Grove, 2000
36 Suess M, Grafmüller B, Zahn R. A novel high resolution, wide swath SAR system. In: Proc of IEEE International Geoscience and Remoye Sensing Symposium (IGARSS), Sydney, 2001. 1013–1015
37 Suess M. Side-Looking Synthetic Aperture Radar System. European Patent 1,241,487. 2006
38 Currie A, Brown M A. Wide-swath SAR. IEE Proc F Radar Signal Process, 1992, 139: 122–135
39 Elad M. Sparse and Redundant Representations: From Theory to Applications in Signal and Image Processing. New York: Springer, 2010
40 Mallat S G, Zhang Z. Matching pursuits with time-frequency dictionaries. IEEE Trans Signal Process, 1993, 41: 3397–3415
41 Chen S S, Donoho D L, Saunders M A. Atomic decomposition by basis pursuit. SIAM J Sci Comput, 1999, 20: 33–61
42 Candès E J, Tao T. Decoding by linear programming. IEEE Trans Inf Theory, 2005, 51: 4203–4215
43 Candès E, Tao T. The Dantzig selector: Statistical estimation when p is much larger than n. The Annal Stat, 2007, 35: 2313–2351
44 Candès E J, Romberg J, Tao T. Robust uncertainty principles: Exact signal reconstruction from highly incomplete frequency information. IEEE Trans Inf Theory, 2006, 52: 489–509
45 Candès E, Romberg J. Sparsity and incoherence in compressive sampling. Inverse Problem, 2007, 23: 969–985
46 Tsaig Y, Donoho D L. Extensions of compressed sensing. Signal Process, 2006, 86: 549–571
47 Baraniuk R G. More is less: Signal processing and the data deluge. Science, 2011, 331: 717–719
48 Baron D, Wakin M B, Duarte M F, et al. Distributed Compressed Sensing. Technical Report. Rice: Rice University, 2005, http://dsp.rice.edu/cs/
49 Duarte M F, Sarvotham S, Baron D, et al. Distributed compressed sensing of jointly sparse signals. In: Conference Record of Asilomar Conference on Signals, Systems and Computers (ACSSC), Pacific Grove, 2005. 1537–1541
50 Zhang Z, Zhang B C, Hong W, et al. Waveform design for Lq regularization based radar imaging and an approach to radar imaging with non-moving platform. In: Proc of European Conference on Synthetic Aperture Radar (EuSAR), Nuremberg, 2012
51 Ahmed N, Natarajan T, Rao K R. Discrete cosine transform. IEEE Trans Comput, 1974, 100: 90–93
52 Daubechies I. Ten Lectures on Wavelets. Philadelphia: SIAM Publications, 2006
53 Ron A, Shen Z. Affine systems in $L_2(d)$: the analysis of the Analysis operator. J Function Analys, 1997,148: 408–447
54 Velisavljevic V, Dragotti P L, Vetterli M. Directional wavelet transforms and frames. In: Proc of Int Conf Image Processing, Rochester, 2002. 589–592
55 Candès E J. Curvelets: A Surprisingly Effective Nonadaptive Representation for Objects with Edges. Technical Report. DTIC Document, 2000. www.curvelet.org/papers/Curve99.pdf

56 Olshausen B A, Field D J. Emergence of simple-cell receptive field properties by learning a sparse code for natural images. Nature, 1996, 381: 607–609

57 Oliver C, Quegan S. Understanding Synthetic Aperture Radar Images. Raleigh: SciTech Publishing, 2004

58 Tian Y, Jiang C L, Lin Y G, et al. An evaluation method for sparse microwave imaging radar system using phase diagrams. In: Proc of CIE Radar Conference, Chengdu, 2011

59 Zhang B C, Jiang H, Hong W, et al. Synthetic aperture radar imaging of sparse targets via compressed sensing. In: Proc of 8th European Conference on Synthetic Aperture Radar (EUSAR), Aachen, 2010

60 Jiang H, Zhang B C, Lin Y G, et al. Random noise SAR based on compressed sensing. In: Proc of IEEE International Geoscience and Remote Sensing Symposium (IGARSS), Honolulu, 2010. 4624–4627

61 Shastry M C, Narayanan R M, Rangaswamy M. Compressive radar imaging using white stochastic waveforms. In: Proc of International Waveform Diversity and Design Conference (WDD), Niagara Falls, 2010. 90–94

62 Bahai A R S, Saltzberg B R, Ergen M. Multi-Carrier Digital Communications: Theory and Applications of OFDM. New York, NY: Springer Science and Business Media Inc, 2004

63 Berger C R, Zhou S, Willett P, et al. Compressed sensing for OFDM/MIMO radar. In: Conference Record of Asilomar Conference on Signals, Systems and Computers (ACSSC), Pacific Grove, 2008. 213–217

64 Berger C R, Demissie B, Heckenbach J, et al. Signal processing for passive radar using OFDM waveforms. IEEE J Sel Top Signal Process, 2010, 4: 226–238

65 Vetterli M, Marziliano P, Blu T. Sampling signals with finite rate of innovation. IEEE Trans Signal Process, 2002, 50: 1417–1428

66 Healy D. Analog-to-Information (A-to-I). 2005. http://www.darpa.mil/mto/solicitations/baa05-35/s/index.html. dARPA/MTO Broad Agency Announcement (BAA) #05-35

67 Healy D, Brady D J. Compression at the physical interface. IEEE Signal Process Mag, 2008, 25: 67–71

68 Laska J N, Kirolos S, Duarte M F, et al. Theory and implementation of an analog-to-information converter using random demodulation. In: Proc of IEEE International Symposium on Circuits and Systems (ISCAS), New Orleans, 2007. 1959–1962

69 Eldar Y C. Compressed Sensing of Analog Signals. Comput Res Reposit, 2008

70 Mishali M, Eldar Y C, Elron A. Xampling, Part I: Practice. ArXiv:09110519. 2009. http://arxiv.org/pdf/0911.0519v3

71 Mishali M, Eldar Y C. From theory to practice: Sub-Nyquist sampling of sparse wideband analog signals. IEEE J Sel Top Signal Process, 2010, 4: 375–391

72 Mishali M, Eldar Y, Dounaevsky O, et al. Xampling: Analog to digital at sub-Nyquist rates. IET Circ Dev Syst, 2011, 5: 8–20

73 Mishali M, Eldar Y C. Xampling: Compressed sensing of analog signals. ArXiv:11032960. 2011. http://arxiv.org/pdf/1103.2960

74 Tropp J A, Laska J N, Duarte M F, et al. Beyond Nyquist: Efficient sampling of sparse bandlimited signals. IEEE Trans Inf Theory, 2010, 56: 520–544

75 Balakrishnan A. On the problem of time jitter in sampling. IRE Trans Inform Theory, 1962, 8: 226–236

76 Sun J P, Zhang Y X, Chen Z B, et al. A novel spaceborne SAR wide-swath imaging approach based on Poisson disk-like nonuniform sampling and compressive sensing. Sci China Inf Sci, 2012, 55: 1876–1887

77 Candès E J, Wakin M B. An introduction to compressive sampling. IEEE Signal Process Mag, 2008, 25, 2: 21–30

78 Carrara W G, Goodman R S, Majewski R M. Spotlight Synthetic Aperture Radar- Signal Processing Algorithms. Norwood, 1995

79 Belcher D P, Baker C J. High resolution processing of hybrid strip-map/spotlight mode SAR. IEE Proc Radar Sonar Nav, 1996, 143: 366–374

80 Mittermayer J, Lord R, Borner E. Sliding spotlight SAR processing for TerraSAR-X using a new formulation of the extended chirp scaling algorithm. In: Proc of IEEE International Geoscience and Remote Sensing Symposium (IGARSS), Toulouse, 2003. 1462–1464

81 De Zan F, Guarnieri A M. TOPSAR: Terrain observation by progressive scans. IEEE Trans Geosci Remote Sens, 2006, 44: 2352–2360

82 Tropp J A, Wright S J. Computational methods for sparse solution of linear inverse problems. Proc IEEE, 2010, 98: 948–958

83 Kim S J, Koh K, Lustig M, et al. An interior-point method for large-scale l1-regularized least squares. IEEE J Sel Top Signal Process, 2007, 1: 606–617

84 Candès E, Romberg J. l1-magic: Recovery of sparse signals via convex Programming. 2005. www.acm.caltech.edu/l1magic/downloads/l1magic.pdf

85 Figueiredo M A T, Nowak R D, Wright S J. Gradient projection for sparse reconstruction: Application to compressed sensing and other inverse problems. IEEE J Sel Top Signal Process, 2007, 1: 586–597

86 Van Den Berg E, Friedlander M. Probing the Pareto frontier for basis pursuit solutions. SIAM J Sci Comput, 2008, 31: 890–912

87 Daubechies I, Defrise M, De Mol C. An iterative thresholding algorithm for linear inverse problems with a sparsity constraint. Commun Pure Appl Math, 2004, 57: 1413–1457

88 Bioucas-Dias J M, Figueiredo M A T. Two-step algorithms for linear inverse problems with non-quadratic regularization. In: Proc of IEEE Int Conf Image Processing, San Antonio, 2007

89 Beck A, Teboulle M. A fast iterative shrinkage-thresholding algorithm for linear inverse problems. SIAM J Imag Sci, 2009, 2: 183–202

90 Yin W, Osher S, Goldfarb D, et al. Bregman iterative algorithms for L1-minimization with applications to compressed sensing. SIAM J Imag Sci, 2008, 1: 143–168

91 Hale E T, Yin W, Zhang Y. Fixed-point continuation for L1 minimization: methodology and convergence. SIAM J Optim, 2008: 1107–1130

92 Hale E T, Yin W, Zhang Y. Fixed-point continuation applied to compressed sensing: implementation and numerical experiments. J Comput Math, 2010, 28: 170–194

93 Becker S, Bobin J, Candès E. NESTA: A fast and accurate first-order method for sparse recovery. ArXiv: 09043367, 2009. http://arxiv.org/pdf/0904.3367

94 Becker S R, Candès E J, Grant M C. Templates for convex cone problems with applications to sparse signal recovery. Math Program Comput, 2011, 3: 165–218

95 Yang J, Zhang Y. Alternating direction algorithms for ℓ_1-problems in compressive sensing. ArXiv:09121185, 2009. http://arxiv.org/pdf/0912.1185

96 Lu Z, Pong T K, Zhang Y. An Method for Finding Dantzig Selectors. ArXiv: 10114604, 2010. http://arxiv.org/pdf/1011.4604

97 Davenport M A, Duarte M F, Eldar Y C, et al. Chapter I: Introduction to compressed sensing. In: Compressed Sensing: Theory and Applications. Cambridge: Cambridge University Press, 2012

98 Tropp J A, Gilbert A C. Signal recovery from random measurements via orthogonal matching pursuit. IEEE Trans Inf Theory, 2007, 53: 4655–4666

99 Donoho D L, Drori I, Tsaig Y, et al. Sparse Solution of Underdetermined Linear Equations by Stagewise Orthogonal Matching Pursuit. Technical Report. Department of Statistics, Stanford University, 2006. http://nmetis.dk/pic/Speciale/HenrikPedersen/Henrik%20Pederse%ns%20Artikler/Compressed%20Sensing/Donoho.pdf

100 Blumensath T, Davies M E. Gradient pursuits. IEEE Trans Signal Process, 2008, 56: 2370–2382

101 Dai W, Milenkovic O. Subspace pursuit for compressive sensing signal reconstruction. IEEE Trans Inf Theory, 2009, 55: 2230–2249

102 Needell D, Vershynin R. Signal recovery from incomplete and inaccurate measurements via regularized orthogonal matching pursuit. IEEE J Sel Top Signal Process, 2010, 4: 310–316

103 Needell D, Tropp J A. CoSaMP: Iterative signal recovery from incomplete and inaccurate samples. Appl Comput Harmon Analys, 2009, 26: 301–321

104 Blumensath T, Davies M E. Iterative hard thresholding for compressed sensing. Appl Comput Harmon Analys, 2009, 27: 265–274

105 Chartrand R. Exact reconstruction of sparse signals via nonconvex minimization. IEEE Signal Process Lett, 2007, 14: 707–710

106 Rao B D, Kreutz-Delgado K. An affine scaling methodology for best basis selection. IEEE Trans Signal Process, 1999, 47: 187–200

107 Chartrand R, Yin W. Iteratively reweighted algorithms for compressive sensing. In: Conference Record of Asilomar Conference on Signals, Systems and Computers (ACSSC), Pacific Grove, 2008. 3869–3872

108 Daubechies I, DeVore R, Fornasier M, et al. Iteratively reweighted least squares minimization for sparse recovery. Commun Pure Appl Math, 2010, 63: 1–38

109 Krishnan D, Fergus R. Fast image deconvolution using hyper-Laplacian priors. In: Advances in Neural Information Processing Systems (NIPS), 2009. 1033–1041

110 Xu Z B, Zhang H, Wang Y, et al. $L_{1/2}$ regularizer. Sci China Inf Sci, 2010, 53: 1159–1169

111 Wipf D P, Rao B D. Sparse Bayesian learning for basis selection. IEEE Trans Signal Process, 2004, 52: 2153–2164

112 Ji S, Xue Y, Carin L. Bayesian compressive sensing. IEEE Trans Signal Process, 2008, 56: 2346–2356

113 Ji S, Dunson D, Carin L. Multitask compressive sensing. IEEE Trans Signal Process, 2009, 57: 92–106

114 Babacan S D, Mancera L, Molina R, et al. Non-convex priors in Bayesian compressed sensing. In: Proc of 17th European Signal Processing Conference (EUSIPCO), Glasgow, 2009

115 Yoon Y S, Amin M G. Compressed sensing technique for high-resolution radar imaging. In: Proc SPIE, 2008. 6968

116 Stojanovic I, Karl W C, Çetin M. Compressed sensing of monostatic and multistatic SAR. In: Proc SPIE, 2009. 7337

117 Huang Q, Qu L, Wu B, et al. UWB through-wall imaging based on compressive sensing. IEEE Trans Geosci Remote Sens, 2010, 48: 1408–1415

118 Jiang C L, Jiang H, Zhang B C, et al. SNR analysis for SAR imaging from raw data via compressed sensing. In: Proc of European Conference on Synthetic Aperture Radar (EUSAR), Nuremberg, 2012

119 Austin C D, Ertin E, Moses R L. Sparse Multipass 3D SAR imaging: applications to the GOTCHA data set. In: Proc SPIE, 2009. 7337

120 Zhang L, Xing M, Qiu C W, et al. Resolution enhancement for inversed synthetic aperture radar imaging under low SNR via improved compressive sensing. IEEE Trans Geosci Remote Sens, 2010. 48, 10: 3824–3838

121 Xie X C, Zhang Y H. High-resolution imaging of moving train by ground-based radar with compressive sensing. Electron Lett, 2010, 46: 529–531

122 Alonso M T, López-Dekker P, Mallorqui J J. A novel strategy for radar imaging based on compressive sensing. IEEE Trans Geosci Remote Sens, 2010, 48: 4285–4295

123 Wu Y R, Xu Z B, Hong W, et al. Sparse SAR Imaging Algorithm based on SAR Raw Data Simulator (in Chinese). China Patent, 201110182202.9. 2012

124 Andrecut M. Fast GPU implementation of sparse signal recovery from random projections. ArXiv: 08091833, 2008. http://arxiv.org/pdf/0809.1833

125 Borghi A, Darbon J, Peyronnet S, et al. A Simple Compressive Sensing Algorithm for Parallel Many-Core Architectures. Technical Report. 2008. http://www-micrel.deis.unibo.it/benini/files/MD/cam08-64.pdf

126 Liu B, Zou Y M, Ying L. SparseSENSE: application of compressed sensing in parallel MRI. In: Proc of International Conference on Information Technology and Applications in Biomedicine (ITAB), Shenzhen, 2008. 127–130

127 Chang C H, Ji J. Compressed sensing MRI with multichannel data using multicore processors. Magn Reson Med, 2010, 64: 1135–1139

128 Tropp J A. Greed is good: Algorithmic results for sparse approximation. IEEE Trans Inf Theory, 2004, 50: 2231–2242

129 Ben-Haim Z, Eldar Y C, Elad M. Coherence-based performance guarantees for estimating a sparse vector under random noise. IEEE Trans Signal Process, 2010, 58: 5030–5043

130 Stanley H E. Introduction to Phase Transitions and Critical Phenomena. Oxford: Oxford Press, 1987

131 Donoho D, Stodden V. Breakdown point of model selection when the number of variables exceeds the number of observations. In: Proc of IEEE International Joint Conference on Neural Network (IJCNN), Vancouver, 2006. 1916–1921

132 Donoho D L, Tsaig Y. Fast Solution of L1-Norm Minimization Problems When the Solution May Be Sparse. Technical Report. Dept. of Statistics, Stanford University, 2006. http://www-dsp.rice.edu/files/cs/FastL1.pdf

133 Donoho D, Tanner J. Observed universality of phase transitions in high-dimensional geometry, with implications for modern data analysis and signal processing. Philosoph Trans Royal Soc A Math Phys Engin Sci, 2009, 367: 4273–4293

134 Donoho D, Jin J. Feature selection by higher criticism thresholding achieves the optimal phase diagram. Philosoph Trans Royal Soc A Math Phys Engin Sci, 2009, 367: 4449–4470

135 Zhu X X, Bamler R. Super-resolution power and robustness of compressive sensing for spectral estimation with application to spaceborne tomographic SAR. IEEE Trans Geosci Remote Sens, 2012, 50: 247–258

136 Herman M A, Strohmer T. High-resolution radar via compressed sensing. IEEE Trans Signal Process, 2009, 57: 2275–2284

137 Jiang H. Study on Processing Algorithm and Analysis of Imaging Performance of Compressed Sensing Radar via Information Theory. Master's thesis. Beijing: Institute of Electronics, Chinese Academy of Sciences, 2011

138 Jiang C L, Zhang B C, Zhang Z, et al. Experimental results and analysis of Sparse Microwave Imaging from spaceborne radar raw data. Sci China Inf Sci, 2012, 55: 1801–1815

139 Zhang B C, Hong W, Wu Y R, et al. A Radar Imaging Azimuth Ambiguity Reducing Method Based on ℓ_q Regularization (in Chinese). China Patent, 201110310655.5. 2012.

140 Lin Y G, Zhang B C, Jiang H, et al. Multi-channel SAR imaging based on distributed compressive sensing. Sci China Inf Sci, 2012, 55: 245–259

141 Lin Y G, Zhang B C, Hong W, et al. Along-track interferometric SAR imaging based on distributed compressed sensing. Electron Lett, 2010, 46: 85–860

142 Lin Y G. Study on Multi-channel SAR Imaging Based on Compressive Sensing. Ph.D. thesis. Beijing: Institute of Electronics, Chinese Academy of Sciences, 2011

143 Farhat N H, Werner C L, Chu T H. Prospects for three-dimensional projective and tomographic imaging radar networks. Radio Sci, 1984, 19: 1347–1355

144 Mahafza B R, Sajjadi M. Three-dimensional SAR imaging using linear array in transverse motion. IEEE Trans Aerosp Electron Syst, 1996, 32: 499–510

145 Reigber A, Moreira A. First demonstration of airborne SAR tomography using multibaseline L-band data. IEEE Trans Geosci Remote Sens, 2000, 38: 2142–2152

146 Zhu X X, Bamler R. Tomographic SAR inversion by L1-norm regularization – the compressive sensing approach. IEEE Trans Geosci Remote Sens, 2010, 48: 3839–3846

147 Baselice F, Ferraioli G, Pascazio V. Three dimensional reconstruction using COSMO-SkyMed high-resolution data. In: Proceedings of Microwaves, Radar and Remote Sensing Symposium (MRRS), 2011. 161–164

148 Budillon A, Evangelista A, Schirinzi G. Three-dimensional SAR focusing from multipass signals using compressive sampling. IEEE Trans Geosci Remote Sens, 2011, 49: 488–499
149 Zhu X X, Bamler R. Very High Resolution SAR tomography via compressive sensing. In: Proc of Fringe Workshop Advances in the Science and Applications of SAR Interferometry, Frascati, 2009
150 Zhu X X, Bamler R. Compressive sensing for high resolution differential SAR tomography-the SL1MMER algorithm. In: Proceedings of IEEE International Geoscience and Remote Sensing Symposium (IGARSS), Honolulu, 2010. 17–20
151 Zhu X X, Bamler R. Within the resolution cell: Super-resolution in tomographic SAR imaging. In: Proc of IEEE International Geoscience and Remote Sensing Symposium (IGARSS), Vancouver, 2011. 2401–2404
152 Zhu X X, Bamler R. Demonstration of Super-Resolution for Tomographic SAR Imaging in Urban Environment. IEEE Trans Geosci Remote Sens, 2012, in press
153 Khomchuk P, Bilik I, Kasilingam D. Compressive sensing-based SAR tomography. In: Proc of IEEE Radar Conference, Washington, 2010. 354–358
154 Tan W X. Study on Theory and Algorithms for Three-Dimensional Synthetic Aperture Radar Imaging. Ph.D. thesis. Beijing: Institute of Electronics, Chinese Academy of Science, 2009
155 Wehner D R. High Resolution Radar. Norwood: Artech House Inc, 1987
156 Zhang L, Xing M, Qiu C W, et al. Achieving higher resolution ISAR imaging with limited pulses via compressed sampling. IEEE Geosci Remote Sens Lett, 2009, 6: 567–71
157 Wang H, Quan Y, Xing M, et al. ISAR imaging via sparse probing frequencies. IEEE Geosci Remote Sens Lett, 2011, 8: 451–455
158 Zhang L, Qiao Z, Xing M, et al. High-resolution ISAR imaging with sparse stepped-frequency waveforms. IEEE Trans Geosci Remote Sens, 2011, 49: 4630–4651
159 Lei Z, Qiao Z, Xing M, et al. High resolution ISAR imaging by exploiting sparse apertures. IEEE Trans Anten Propag, 2011, 60: 997–1008
160 Zhu F, Zhang Q, Xiang Y, et al. Compressive Sensing in ISAR spectrogram data transmission. In: Proc of Asian-Pacific Conference on Synthetic Aperture Radar (APSAR), Xi'an, 2009. 89–92
161 Zhu F, Zhang Q, Lei Q, et al. Reconstruction of moving target's HRRP using sparse frequency-stepped chirp signal. IEEE Sensors J, 2011, 11: 2327–2334
162 Ye F, Liang D, Zhu J. ISAR enhancement technology based on compressed sensing. Electron Lett, 2011, 47: 620–621
163 Rao W, Li G, Wang X, et al. ISAR imaging of uniformly rotating targets via parametric weighted L1 minimization. In: Proc of Asian-Pacific Conference on Synthetic Aperture Radar (APSAR), Seoul, 2011
164 Daniels D J. Surface-penetrating radar. Electron Commun Engin J, 1996, 8: 165–182
165 Daniels D J. Ground Penetrating Radar. Herts: The Institution of Engineering and Technology, 2004
166 Gurbuz A C, McClellan J H, Scott W R. Compressive sensing for subsurface imaging using ground penetrating radar. Signal Process, 2009, 89: 1959–1972
167 Feng X, Sato M. Pre-stack migration applied to GPR for landmine detection. Inverse Problem, 2004, 20: S99
168 Stolt R H. Migration by Fourier transform. Geophysics, 1978, 43: 23–48
169 Gurbuz A C, McClellan J H, Scott W R. Compressive sensing for GPR imaging. In: Conference Record of Asilomar Conference on Signals, Systems and Computers (ACSSC), Pacific Grove, 2007. 2223–2227
170 Gurbuz A C, McClellan J H, Scott W R. GPR imaging using compressed measurements. In: Proc of IEEE International Geoscience and Remote Sensing Symposium (IGARSS), Boston, 2008. 11–13
171 Suksmono A B, Bharata E, Lestari A A, et al. A compressive SFCW-GPR system. In: Proc of 12th Int Conf on Ground Penet Radar, Birmingham, 2008. 16–19
172 Suksmono A B, Bharata E, Lestari A A, et al. Compressive stepped-frequency continuous-wave ground-penetrating radar. IEEE Geosci Remote Sens Lett, 2010, 7: 665–669
173 Gurbuz A C, McClellan J H, Scott W R. A compressive sensing data acquisition and imaging method for stepped frequency GPRs. IEEE Trans Signal Process, 2009, 57: 2640–2650
174 Soldovieri F, Solimene R, Ahmad F. A fast data acquisition and processing scheme for through-the-wall radar imaging. In: Proc SPIE, 2011. 8021
175 Varshney K R, Çetin M, Fisher III J W, et al. Joint image formation and anisotropy characterization in wide-angle SAR. In: Proc SPIE, 2006. 6237
176 Stojanovic I, Çetin M, Karl W C. Joint space aspect reconstruction of wide-angle SAR exploiting sparsity. In: Proceedings of SPIE, 2008. 6970
177 Soumekh M. Reconnaissance with slant plane circular SAR imaging. IEEE Trans Image Process, 1996, 5: 1252–1265
178 Potter L C, Ertin E, Parker J T, et al. Sparsity and compressed sensing in radar imaging. Proc IEEE, 2010, 98: 1006–1020
179 Lin Y, Hong W, Tan W X, et al. Compressed sensing technique for circular SAR imaging. In: Proc of IET International Radar Conference, Guilin, 2009
180 Lin Y. Study on Algorithms for Circular Synthetic Aperture Radar Imaging. Ph.D. thesis. Beijing: Institute of

Electronics, Chinese Academy of Sciences, 2011
181 Fishler E, Haimovich A, Blum R, et al. MIMO radar: An idea whose time has come. In: Proc of IEEE Radar Conference, Philadelphia, 2004. 71–78
182 Li J, Stoica P. MIMO Radar Signal Processing. Hoboken: Wiley, 2009
183 Bliss D W, Forsythe K W. Multiple-input multiple-output (MIMO) radar and imaging: degrees of freedom and resolution. In: Conference Record of Asilomar Conference on Signals, Systems and Computers (ACSSC), Pacific Grove, 2003. 54–59
184 Chen C Y, Vaidyanathan P P. Compressed sensing in MIMO radar. In: Conference Record of Asilomar Conference on Signals, Systems and Computers (ACSSC), Pacific Grove, 2008. 41–44
185 Strohmer T, Friedlander B. Compressed sensing for MIMO radar-algorithms and performance. In: Conference Record of Asilomar Conference on Signals, Systems and Computers (ACSSC), Pacific Grove, 2009. 464–468
186 Petropulu A P, Yu Y, Poor H V. Distributed MIMO radar using compressive sampling. In: Conference Record of Asilomar Conference on Signals, Systems and Computers (ACSSC), Pacific Grove, 2008. 203–207
187 Yu Y, Petropulu A, Poor H V. MIMO radar using compressive sampling. IEEE J Sel Top Signal Process, 2010, 4: 146–163
188 Yu Y, Petropulu A, Poor H. Measurement matrix design for compressive sensing based MIMO radar. IEEE Trans Signal Process, 2011, 59: 5338–5352
189 Gogineni S, Nehorai A. Target estimation using sparse modeling for distributed MIMO radar. IEEE Trans Signal Process, 2011, 59: 5315–5325
190 Tan X, Roberts W, Li J, et al. Sparse learning via iterative minimization with application to MIMO radar imaging. IEEE Trans Signal Process, 2011, 59: 1088–1101
191 Berger C R, Zhou S, Willett P. Signal extraction using compressed sensing for passive radar with OFDM signals. In: Proc of 11th International Conference on Information Fusion, Cologne, 2008
192 Xu H, He X, Yin Z, et al. Compressive sensing MIMO radar imaging based on inverse scattering model. In: Proc of IEEE International Conference on Signal Processing (ICSP), Beijing, 2010. 1999–2002
193 Wang J, Li G, Zhang H, et al. SAR Imaging of Moving Targets via Compressive Sensing. ArXiv: 11041074, 2011. http://arxiv.org/pdf/1104.1074
194 Khwaja A S, Ma J. Applications of compressed sensing for SAR moving-target velocity estimation and image compression. IEEE Trans Instrum Meas, 2011, 60: 2848–2860
195 Stojanovic I, Karl W C. Imaging of moving targets with multi-static SAR using an overcomplete dictionary. IEEE J Sel Top Signal Process, 2010, 4: 164–176
196 Ferrara M, Jackson J, Stuff M. Three-dimensional sparse-aperture moving-target imaging. In: Proceedings of SPIE, 2008. 6970
197 Benz U, Strodl K, Moreira A. A comparison of several algorithms for SAR raw data compression. IEEE Trans Geosci Remote Sens, 1995, 33: 1266–1276
198 Kwok R, Johnson W. Block adaptive quantization of Magellan SAR data. IEEE Trans Geosci Remote Sens, 1989, 27: 375–383
199 Bhattacharya S, Blumensath T, Mulgrew B, et al. Fast encoding of synthetic aperture radar raw data using compressed sensing. In: Proc of 14th IEEE Workshop on Statistical Signal Processing, Madison, 2007. 448–452
200 Bhattacharya S, Blumensath T, Mulgrew B, et al. Synthetic aperture radar raw data encoding using compressed sensing. In: Proc of IEEE Radar Conference, Rome, 2008
201 Sarvotham S, Baron D, Baraniuk R G. Measurements vs. bits: Compressed sensing meets information theory. In: Proc of 44th Allerton Conf Comm Ctrl Computing, Monticello, 2006
202 Wainwright M J. Information-theoretic limits on sparsity recovery in the high-dimensional and noisy setting. IEEE Trans Inf Theory, 2009, 55: 5728–5741
203 Aeron S, Saligrama V, Zhao M. Information theoretic bounds for compressed sensing. IEEE Trans Inf Theory, 2010, 56: 5111–5130